Komatiites From Mantle Transition Zone Plumes

Derek Wyman*

School of Geosciences, The University of Sydney, Sydney, NSW, Australia

During the Archean, episodic volcanism commonly included both plume- and arc-type magmatism, raising the issue of a possible link between "bottom up" and "top down" geodynamic processes. Rather than plume-initiated subduction, the best-preserved cratons demonstrate that komatiitic magmatism postdated at least some of the subduction linked volcanism. Several factors suggest that komatiite-generating plumes were sourced in the mantle transition zone. Komatiites contain 0.6 wt.% or more H_2O, which is contrary to earlier predictions for plume ascent through the transition zone. Geodynamic reconstructions indicate that multiple subducted slabs penetrated the transition zone in the region of future plume ascent and the related trench configurations limit the size of any associated plume heads. The implied plume head sizes are inconsistent with those required for a plume to ascend from the core-mantle boundary but match those predicted for plumes sourced from the lower transition zone. Transition zone plumes have mainly been advocated for in post-Archean "big wedge" scenarios involving subducted slabs that stall at the base of the transition zone but they are also an outcome of the "basalt barrier" featured in some geodynamic models for the Archean and early Proterozoic. The latter models suggest the basaltic components of Archean subducted slabs were too buoyant to descend into the lower mantle and formed a boundary layer that isolated the upper mantle and lower mantle on the early Earth, except in times of mantle overturns. The basalt barrier was a significant thermal boundary layer that, in principle, could act as the nucleation site of upwelling plumes anywhere on the globe. The evidence discussed here, however, suggests that the mainly peridotitic mantle upwellings were enhanced by the nearby injection of closely associated slabs into the transition zone. The simplicity of the Mantle Transition Zone (MTZ) plume-forming mechanism ensured that komatiites could be generated throughout the Archean even as Earth moved toward a regime involving modern-style subduction, globe-encompassing oceanic ridge systems and tectonic plates. The distinctive geodynamic setting of Gorgona Island produced relatively low-temperature komatiites at the only place along the margin of North and South America where it was possible to reproduce the bowl-like subduction configurations commonly associated with their Archean and Paleoproterozoic counter parts.

Keywords: Archean, cratons, transition zone, komatiite, mantle plume

INTRODUCTION

Recent years have seen significant advances in the quality of mantle plume imaging, the sophistication of numerical models for the upwellings themselves and their interaction with tectonic plates (Mittelstaedt and Ito, 2005; Bredow et al., 2017; Nelson and Grand, 2018). A wide range of plume types have been suggested, including shallow and deep types (Courtillot et al., 2003), sheet-like and pulsating varieties (Mjelde et al., 2010; Namiki et al., 2013) that only rarely define simple symmetrical upwellings (Zhao, 2007). Without the capacity for the direct measurement of Archean plume features, the literature on Archean geodynamics and crustal growth has not witnessed a comparable in-depth re-assessment of the purported craton-forming upwellings from the core – mantle boundary. Geodynamic controversies for this time interval mainly focus on whether an Archean mantle plume scenario is appropriate for a particular terrane or the period in time when mushroom-shaped plumes were joined by recognizable plate tectonic processes. If there is any takeaway from the study of Phanerozoic plumes, however, it is that we must still have much to learn about their older counter parts.

Many commonly held beliefs concerning Archean plumes rest on scant evidence and became entrenched more than 20 years ago. This paper will argue that many features commonly attributed to Archean plume models are difficult to reconcile with each other or with other evidence presented by the geological record. A potential source for komatiites in the Mantle Transition Zone, as suggested by Shimizu et al. (2001) and Wyman (2018), but also implied by some earlier papers (e.g., Davies, 1995, 2008), is explored as a possible means to resolve outstanding issues relating to Archean geodynamics and komatiite genesis from the Paleoarchean to the Phanerozoic.

ARCHEAN PLUME MODELS

Previous Archean Plume Models

Arndt et al. (2008) summarized the evolution of our understanding of komatiites from the early recognition of their distinctive high-Mg volcanic character (Viljoen and Viljoen, 1969) through to progressively more comprehensive major and trace element studies (e.g., Sun and Nesbitt, 1978) and isotopic characterizations (e.g., Sm-Nd: Claoué-Long et al., 1988; Lu-Hf: Gruau et al., 1990). Green et al. (1975) undertook the initial komatiite experimental studies and concluded that the eruption temperature of the studied Barberton greenstone belt sample was 1650 ± 20°C and that its water content was less than 0.2%. As Arndt et al. (2008) also make clear, although controversies regarding komatiite magma water content would sporadically arise, the groundwork for models of dry and hot Archean thermal mantle plumes was established quite early on, based on the high temperatures implicated in these pioneering studies. The alternative view, supporting hydrous komatiite melts, was most forcefully argued in papers such as Grove and Parman (2004) and has persisted with some support ever since.

Campbell and Griffiths (1990, 1992, 1993) noted that there are two possible locations for mantle thermal plumes: the boundaries between upper and lower mantle and between the mantle and core (CMB). Considering factors such as the plume dynamics required to generate ~1000 km plume heads (e.g., high buoyancy flux rates: Courtillot et al., 2003), the (approximately) fixed position of present-day hotspots, and their estimate of modern plume contributions to the Earth's heat budget, they argued that major plumes must originate at the CMB. The conclusion was then transferred to Archean plumes, apparently based on the inferred size of the Yilgarn plume head and their estimate of ~300 km as the maximum diameter for plumes formed in the upper mantle.

The concept that Archean mantle plumes generated komatiites and associated tholeiitic magmas was argued in papers such as Campbell et al. (1989). Their "isochemical" starting plume experiments, involving cool and warm glucose syrup, suggested that komatiites were derived from the plume tail, which was dominated by material rising from the core-mantle boundary, and tholeiitic basalts were derived from the plume head that included significant amounts of entrained upper mantle. Campbell and Hill (1988) suggested a two-stage, mantle plume-driven, model for the granite-greenstone terranes of the Kalgoorlie-Norseman area of the Yilgarn Craton. The model was highly influential for interpretations of Yilgarn evolution and Campbell and Hill (1988) considered it likely to have widespread applicability. Key features of the model included large plume heads (~2000 km diameters or wider after flattening: **Figure 1**) and crustal thinning driven by plume ascent, which facilitated the eruption of shallow mantle magmas that generally underwent ~10% fractionation of olivine. Post-komatiite Yilgarn granites generally display abundant isotopic and xenocrystic evidence for crustal reprocessing, which was accounted for by crustal melting driven by heating of the lithosphere by the underlying flattened plume head. The present granite-greenstone belt geometry was suggested to result from the ascent of the plume-generated felsic magmas to shallow crustal levels.

As observed by Kamber and Tomlinson (2019), among others, the relatively abrupt decline in komatiite production near the end of the Archean was accompanied by significant disruptions in other secular trends such as the styles of felsic magmatism, compositional changes in both clastic and hydrogenous sedimentary rocks, and others. Diverse competing models for the evolution of the Earth's mantle have resulted in multiple explanations for these changes. Campbell and Griffiths (2014) invoke an Archean transition from drip to subduction tectonics. The increasing abundance of subducted slabs allowed for formation of the core-enveloping D" insulating layer, which they link to a step-like drop in maximum magma MgO contents and calculated mantle temperatures between 2.7 and 2.0 Ga. This development also corresponds to the switch from komatiite-bearing plumes to ocean island basalt (OIB)-related post-Archean examples.

An alternative model for the Archean mantle, proposed by Davies (1995, 2008), suggests that there was a "basalt boundary" layer in the upper mantle during the Archean. The boundary developed because subducted basaltic material accumulated at the bottom of the transition zone due to its relative buoyancy
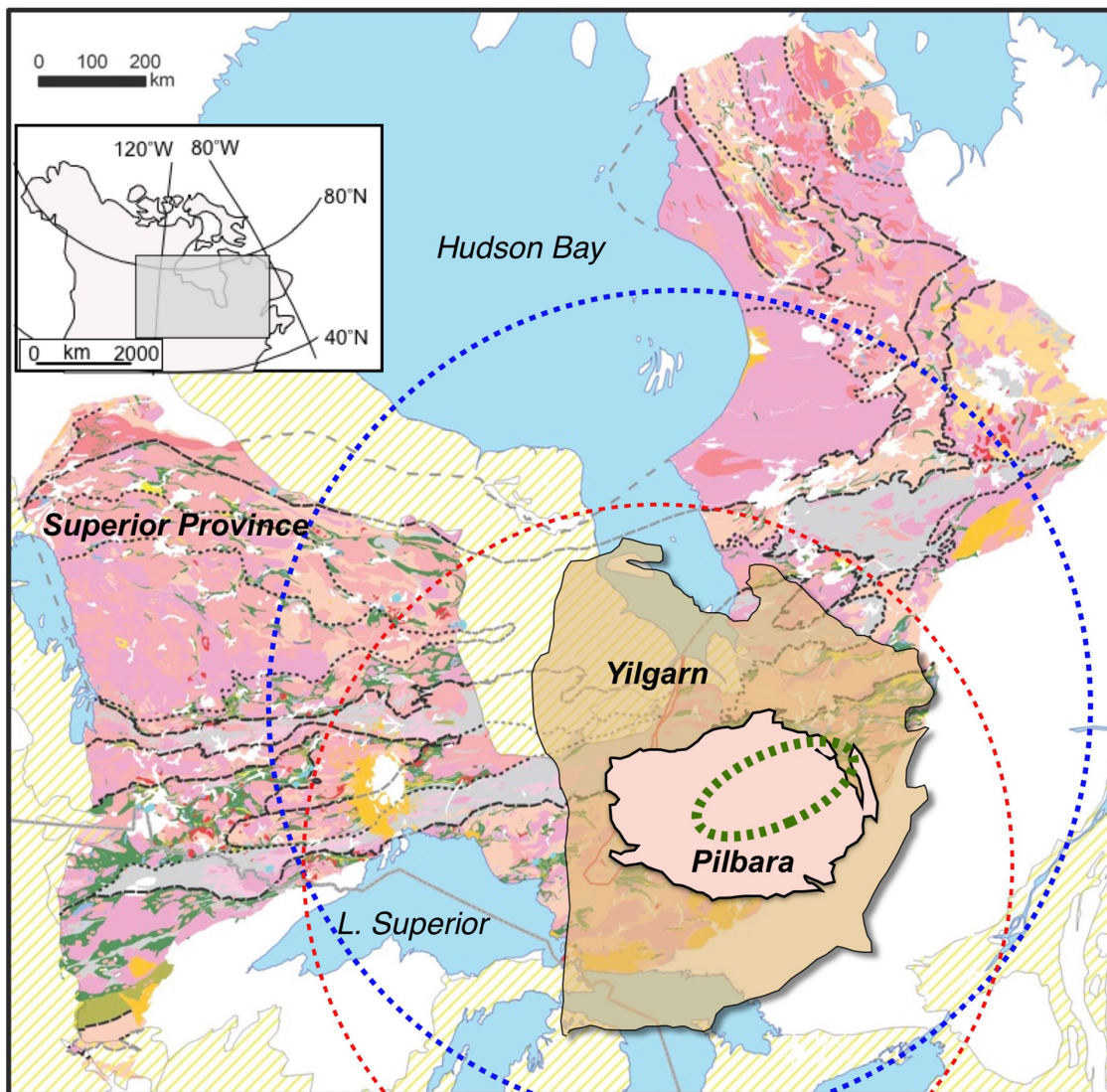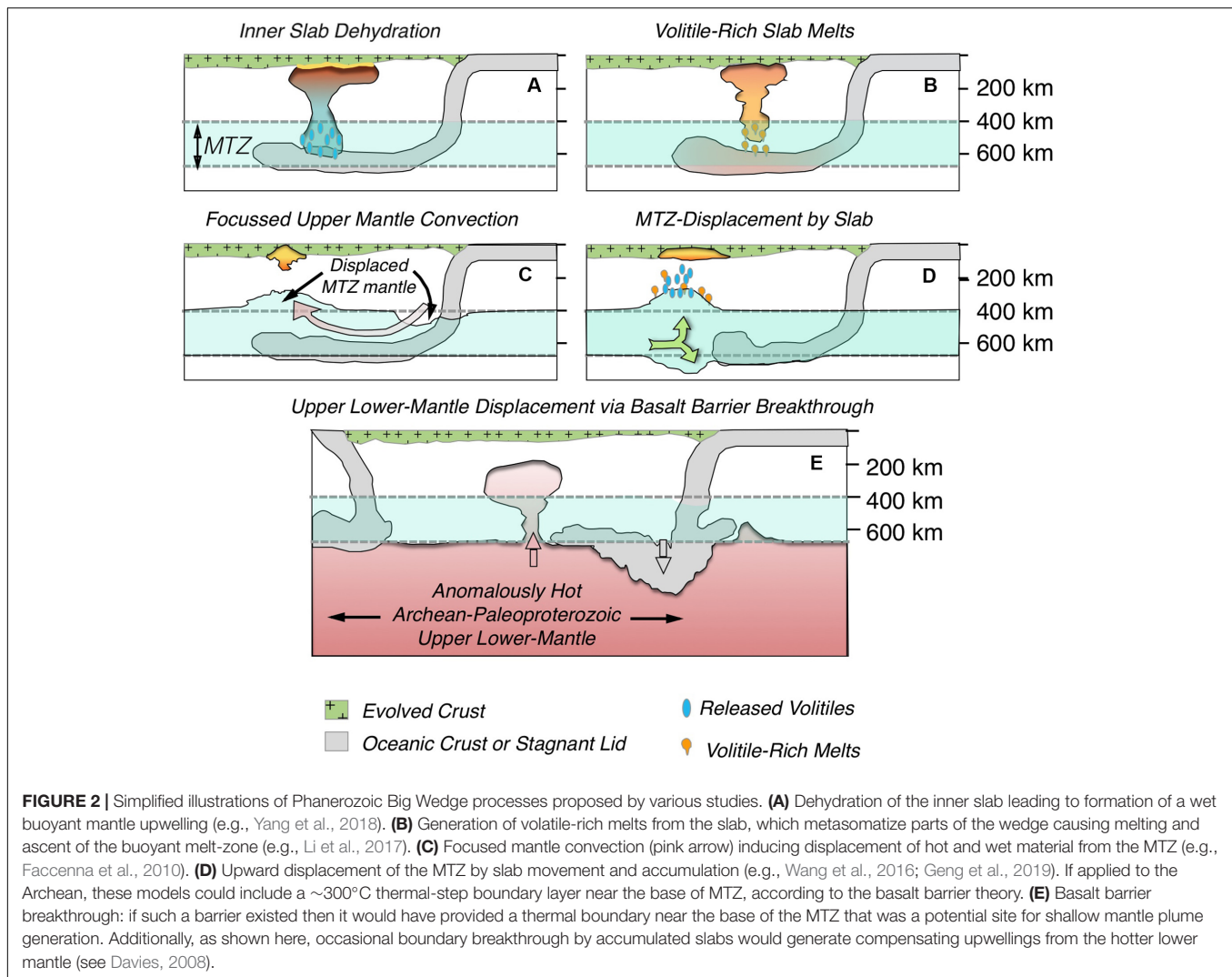
FIGURE 1 | A comparison of the Superior Province, Yilgarn Craton and Pilbara Craton showing the approximate sizes of mantle plume heads as inferred by Mole et al. (2014) for the Yilgarn ~2900 (blue circle) and ~2700 Ma (red circle) plumes and Dostal and Mueller (2013) for the Abitibi. The Abitibi plume is shown as a green dashed ellipse, based on the plume head shape implied in Dostal and Mueller (2013). No size estimates are available for the suggested eight mantle plume events of the 3530–3230 Ma Pilbara Supergroup inferred by Hickman and Van Kranendonk (2012). The historically inferred size of Yilgarn mantle plume heads is inconsistent with Superior Province geological field relations or the Archean plume events ascribed to the craton. See text for a discussion of the plume size estimates. Areas marked with yellow diagonal lines are overlain by Phanerozoic sedimentary cover. Superior Province map from Percival et al. (2012). Location of the Superior Province Craton is shown in the inset. The locations of the Yilgarn and Pilbara Cratons are shown in **Figure 3**.

(vs. peridotite) under the prevailing mantle temperatures. The barrier divided the mantle into two isolated regions, except during episodes of mantle overturn, and prevented subducted oceanic crust from entering the deep mantle while also creating a temperature difference of up to 300°C between the upper and lower mantle at the interface. In the Davies (1995, 2008) models, it is the permanent removal of this upper mantle "basalt barrier" that marks a major geodynamic change during the Paleoproterozoic. The Davies model has very different implications for Archean plumes compared to the scenario favored by Campbell and Griffiths. Although Davies (1995)

indicated that Archean deep mantle CMB plumes may have existed, the upper mantle boundary would have prevented their ascent to surface. Conversely, a temperature contrast between the cooler upper and warmer lower mantle would have facilitated the development of small shallow-mantle plumes that Davies (1995) estimated would have head diameters on the order of 200–300 km. In the models of Davies (2008), breakthroughs of the cooler upper mantle that drain into the lower mantle are accompanied by upward movement of hot lower mantle. Davies (2008) notes that the models are highly generalized, but such breakthroughs could be significant

FIGURE 2 | Simplified illustrations of Phanerozoic Big Wedge processes proposed by various studies. **(A)** Dehydration of the inner slab leading to formation of a wet buoyant mantle upwelling (e.g., Yang et al., 2018). **(B)** Generation of volatile-rich melts from the slab, which metasomatize parts of the wedge causing melting and ascent of the buoyant melt-zone (e.g., Li et al., 2017). **(C)** Focused mantle convection (pink arrow) inducing displacement of hot and wet material from the MTZ (e.g., Faccenna et al., 2010). **(D)** Upward displacement of the MTZ by slab movement and accumulation (e.g., Wang et al., 2016; Geng et al., 2019). If applied to the Archean, these models could include a ~300°C thermal-step boundary layer near the base of MTZ, according to the basalt barrier theory. **(E)** Basalt barrier breakthrough: if such a barrier existed then it would have provided a thermal boundary near the base of the MTZ that was a potential site for shallow mantle plume generation. Additionally, as shown here, occasional boundary breakthrough by accumulated slabs would generate compensating upwellings from the hotter lower mantle (see Davies, 2008).

for Archean plumes given the intrinsic link between the upwellings and subduction.

Big Wedges and Inward-Facing Subduction

The basalt barrier of Davies' (2008) Archean Earth numerical model produces stalled slabs in the upper mantle that are similar to those imaged from seismic data in some present-day subduction zones (Goes et al., 2017), although the younger examples are not associated with such a pronounced thermal boundary at the base of the MTZ. These shallow slab settings are key features in a variety of "big wedge" models that involve recycling of subduction-related material into the MTZ followed by mantle upwelling toward the shallow crust (Maruyama et al., 2009; Zhao et al., 2009; Zhao, 2017). Similar ideas have been proposed by numerous workers to account for specific observations with or without the "big wedge" label (**Figure 2**). Wang et al. (2015) showed that late Cenozoic continental flood basalts, which originated directly above the edge of the Pacific stagnant slab beneath China, could be accounted for by

subducted fluids triggering wet melting. Yu et al. (2017) also provided evidence from seismic tomography for similar events beneath Southeast Asia.

Thermochemical plume models emphasize the importance of both temperature and chemical composition rather than the artificially generated thermal anomalies commonly used to initiate mantle upwelling in numerical models (Farnetani and Samuel, 2005). He et al. (2017) used this approach in their MTZ study and concluded that wet thermochemical plumes can develop off of the top of flat slabs moving along the 660 km boundary. Yang et al.'s (2018) modeling indicates that such upwellings may contribute to the partial melting and loss of continental lithosphere. Long et al. (2019) also employed numerical modeling to examine the role of stagnant slabs and the fate of water in the MTZ from the context of present-day intra-plate volcanism. They argue that any thick (>60 km) hydrated layer formed in the MTZ would not survive over long time scales and would evolve to an upwelling mantle body.

Although many "big wedge" models invoke magmatism induced via the focused loss of slab volatiles, others indicate

that slab movement within the MTZ can also promote intra-plate mantle upwellings. Faccenna et al.'s (2010) numerical modeling predicts that focused mantle return flow upwelling can be generated ahead of a slab as it travels along the 660 km boundary and along slab edges. Volcanism produced ahead of the slab would commonly be located 100's of km inboard of the trench. They argued that slab-induced mantle flow could produce "intraplate off-volcanic arc-volcanism" due to decompression melting that in some cases is assisted by dehydration from the slab. These "subduction-triggered plumes" are distinct from CMB plumes and result from slab-induced upward displacement of volumes of upper mantle. Given that "the melting temperature of the mantle increases with pressure or depth more rapidly than the adiabatic temperature, any small upward displacement of a parcel of upper mantle at or very near its melting temperature will cause decompression melting (p. 64)." Faccenna et al. (2010) also note that the melting creates buoyancy forces that potentially lead to a self-sustaining process of plume generation. These types of big wedge processes alone could not be responsible for the excess temperatures implicated for Archean komatiites, which would require thermal input from the basalt boundary to heat Transition Zone mantle. The big wedge setting, however, can focus upwelling and contribute to the displacement of peridotitic mantle in the vicinity of subduction zones.

Citing examples such as the West Philippine Basin, Faccenna et al. (2010) also considered the special case of inward-facing double subduction where they attribute the development of intra-basin spreading centers and volcanism to slab-driven mantle upwellings. Double subduction zones are potentially of great importance to the global late Archean cratonization event. For example, numerical studies of same-dip double subduction (e.g., 80–50 Ma India – Eurasia: Holt et al. (2017) could clarify the rapid amalgamation of the Superior Province via multiple subduction zones (Percival et al., 2012). Almost unique to studies of the early Earth are circular subduction initiation scenarios around modeled cratons, which are extreme versions of the inward-facing subduction scenario. In some models, it is proposed that mantle plumes provided the impetus for such symmetrical subduction (Ueda et al., 2008). Bolide impacts have also been proposed as the initiators of circular subduction processes (Hansen, 2007). The attributes of pre-existing early Archean proto-cratons, the associated global stagnant lid and contemporaneous mantle processes have been assessed numerically to establish the parameters required for the onset of subduction. Rey et al. (2014) described how the lateral spreading of early continents may have "kick-started" subduction in the adjacent lithosphere. The modeling of Rolf and Tackley (2011) also considered idealized circular cratons in order to establish the effects of stress focusing around the earliest continents. They found that the ratio of cratonic lithosphere thickness vs. oceanic lithosphere was a key factor in determining whether stagnant lid, plate tectonic or episodic stagnant-mobile lid regimes would occur on the early Earth. These studies did not consider the presence of the MTZ or a basalt barrier but inward-facing double subduction zones

or enclosed $\sim$ circular subduction zones likely favor strong mantle upwelling.

Damp Komatiite Models

Shimizu et al. (2001) reported komatiite magma H_2O contents of 0.8–0.9 wt%, based on magma melt inclusion studies in chromites from "unusually fresh" Belingwe greenstone belt samples. They inferred that a hydrous plume from the MTZ was the probable komatiite source. Their results were initially considered suspect (Arndt et al., 2008) but are entirely consistent with the more recent evidence for damp komatiites. For example, Kamenetsky et al. (2010) reported that melt inclusions from Phanerozoic komatiites from Gorgona contained 0.2–1.0 wt% H_2O that required a hydrated mantle source. A classic subduction-modified wedge was not favored, based on the absence of negative Nb anomalies. Subsequently, however, Gurenko and Kamenetsky (2011) reported B isotopic evidence that not only supported the concept of wet komatiites but also suggested that subduction fluids may have been injected into a rising plume.

Based on melt inclusion studies in olivines, Sobolev et al. (2016) reported that the magmas responsible for well-known Archean komatiites in the Abitibi belt contained amounts of water (0.6 wt%) similar to those reported from Gorgona. The water was accounted for by the ascent of a core-mantle boundary plume through the MTZ, thereby allowing for entrainment of the hydrous melt predicted to occur at 410 km by Bercovici and Karato (2003) in their transition zone water filter model. Sobolev et al. (2016) ruled out a supra-subduction environment based on trace element patterns and the low oxygen fugacity of komatiite melts. The geodynamic context of arc-plume interaction associated with the Abitibi komatiites (Ayer et al., 2002; Wyman et al., 2002) was not considered a factor. Similar findings were also reported for 2.7 Ga Belingwe komatiites by Asafov et al. (2018) and for 3.3. Ga Barberton komatiites by Sobolev et al. (2019) who also invoked the MTZ-entrainment model. In a sense, the classic Archean CMB plume model had failed to meet predictions, given that Bercovici and Karato (2003) had suggested they were too big and hot to allow any significant ingress of MTZ water during their ascent.

The results reported by Sobolev et al. (2016) prompted a re-assessment of the Abitibi komatiites by Herzberg (2016), who stated that the volatile-rich komatiites "create ambiguities concerning the thermal properties of the source and all geodynamic interpretations" (p. 2279). Citing the earlier work of Shimizu et al. (2001), he also noted the possibility that the primary magmas had undergone degassing prior to olivine crystallization, which creates significant uncertainties regarding mantle potential temperatures. He tentatively suggested that the volatiles were derived from "wet spots" in either plumes or ambient mantle that they had been sequestered in the mantle since the Hadean.

Wyman (2018) arrived at a model for MTZ-sourced komatiites from three main observations. First, the Archean record for specific cratons, and globally, displays episodic occurrences of volcanism separated by substantial time gaps (10's to 100's of million years), but the volcanic episodes commonly included both plume- and subduction-style rock types, raising

the issue of whether their genesis was closely linked. Second, Late Archean komatiitic volcanism in the Superior Province occurred along the margin of the already amalgamating craton, rather than being consistent with any plume-induced subduction scenario. Third, persistent controversy over the plausibility of Abitibi belt CMB plume-arc interaction, based on space problems linked to CMB plume size and the alternations of plume and arc rock types, requires that the plume models also be scrutinized along with those for Archean subduction. The findings of Sobolev et al. (2016) were taken as evidence that the resolution of these issues could plausibly require that komatiites were derived from plumes that originated in the Transition Zone mantle, which must have far smaller plume heads than CMB plumes, assuming that they resemble classic models at all. This scenario does not conflict with petrological literature on komatiite genesis because their melts develop above the Transition Zone mantle. The key issue is the excess temperatures implicated in their formation and, on this subject, Wyman (2018) referred to the basalt barrier models described by Davies (2008) and Kamber (2015). The remainder of this paper considers recent evidence in support of the damp MTZ plume model and the implications of such a process from Earth's geodynamic evolution since the early Archean.

DISTINGUISHING CMB AND MTZ PLUMES

Criteria Types

Although initially extrapolated from evidence for deep Phanerozoic plumes, the Archean CMB plume hypothesis is well established in the literature, and key predictions have been made concerning the komatiite-associated upwellings. The big wedge literature includes a large array of models but there are recurring features that are characteristic of proposed MTZ

plumes that distinguish them from CMB counterparts. These two sets criteria and those suggested by Wyman (2018) based on the Superior Province as a whole are summarized in **Table 1**.

The temporal and spatial scales required to assess some of the criteria listed in **Table 1** are notable. There are very few cratons where the thermal consequences of a ~2000 km flattened plume head can be assessed. Conversely, all varieties of Phanerozoic big wedge models require millions of years of prior subduction to start the mantle upwelling and the resultant volcanism may be 100's of km distant from contemporaneous arc-style volcanism near the trench (Faccenna et al., 2010). Therefore, we first assess whether big wedge models for the formation of Archean komatiites, based on the criteria in **Table 1**, are applicable to the large and well-studied Yilgarn Craton and Abitibi belt. Following this assessment, the broader implications for komatiite generation through time are considered based on the Paleoarchean East Pilbara, when the basalt barrier should have been at its most effective; the Paleoproterozoic Circum-Superior Belt, formed when the barrier is predicted to still be present but in its waning stages; and the Gorgona Island occurrences where the youngest known komatiitic rocks greatly post-date any possible basalt barrier.

Plume Size

As previously noted, the Yilgarn Craton has been considered the type example of cratonic events associated with a large Archean plume head (Campbell and Hill, 1988). Alternative plume models incorporated into craton geodynamic reconstructions have sometimes been rejected on the basis that they are not consistent with the large-scale flattened plume head implied by the CMB model and "are at the wrong scale by at least an order of magnitude, if not two." (Barnes et al., 2012, p. 731). Such upwellings would, however, be broadly consistent with the maximum ~300 km diameter plume heads of MTZ plumes

TABLE 1 | Distinguishing features of core-mantle boundary and mantle transition zone plume models.

Plume Source:	CMB[a]	MTZ[d]
Size	Plume heads exceed 1000 km radii; flattened heads may be 2000–2500 km.	Plume widths are 200–300 km[a].
Shape	Generally considered mushroom-shaped; the tail and head have distinct compositional and T characteristics.	Irregular shapes commonly inferred; based on links to new spreading centers they may be linear and broadly aligned with subduction zone orientations.
Relationship to subduction	Random, or plumes are instigators of subduction (precede subduction).	Subduction events (possibly episodic and global) precede spatially associated plume events but may coexist with the plumes.
Driving force	Buoyancy related to heating of a deep mantle starting volume.	Buoyancy related to thermo-chemical properties of subduction-modified big mantle wedge and/or upward MTZ displacement initiated by subducted slab.
Thermal consequences for cratons	For plume heads, long term (>40–100 m.y.) reprocessing of cratonic crust and lithosphere.	Models suggest that thermal effects are short-lived or require ongoing subduction.
Relationship to cratonic keels	Cratonic keels linked directly to mantle plumes and komatiitic volcanism[b]	No consistent relationship between plume events and lithosphere evolution, but erosion of lithosphere is possible.
Komatiite water content	<0.5 wt%, unless contaminated by MTZ or 410 km hydrous melt layer[c]	Variable but >0.5 wt.%

[a]CMB plume features and MTZ plume head size mainly from Davies (1995) and Campbell and Griffiths (1990,1992, 1993). [b] Herzberg (1993). [c]Arndt et al. (2008). [d]Mainly sources cited in **Figure 2**.

and with the big wedge concepts now being applied to many Phanerozoic convergent margins.

Yilgarn Plume Dimensions

Many key elements of the Campbell and Hill (1988) model have been retained in more recent Yilgarn papers and, for example, the experiments of Campbell et al. (1989) are cited by Barnes et al. (2012). Mole et al. (2014, 2015) and Barnes et al. (2016) also provide examples of the prevalent Yilgarn plume model, although Mole et al. (2014, 2015) do allow for a minor contribution to the Yilgarn's evolution from subduction processes. For convenience, the mantle plume features described by Mole et al. (2014) and Barnes et al. (2016) can serve as a reference for a theoretical Yilgarn core-mantle boundary plume (**Figure 1**). It has been suggested that two thermal plumes ascended beneath the western Yilgarn at ~2.9 and ~ 2.7 Ga. Their plume heads had estimated diameters on the order of 1600–2000 km. Chemical and isotopic variations in the plume-associated volcanism are attributed to differences in depth of melting enforced by the sub-cratonic lithosphere architecture combined with variable extents of crustal interaction and inheritance from compositionally diverse crustal blocks. In the Eastern Goldfields Superterrane, komatiitic magmatism occurred between 2720 and 2700 Ma and was followed by multiple pulses of felsic activity to 2600 Ma (Mole et al., 2015) that have been attributed to the effects of the mantle plume.

Many workers have argued that there is evidence for subduction or both subduction and plume processes in the eastern Yilgarn (e.g., Begg et al., 2010; Czarnota et al., 2010; Cassidy and Wyche, 2012), although it has been difficult to fully reconcile these models because of the inferred size of the plume head. The ages and approximate locations for inferred subduction events are given in **Figure 3**. Also shown are subduction events reported for the western Yilgarn. Although subduction models had been invoked several decades ago, more recent western Yilgarn geodynamic scenarios have shifted from plume-based (Van Kranendonk et al., 2013) to plume plus subduction (Wyman and Kerrich, 2012) and back toward subduction-only models for the interval between 2830 Ma and ~2700 Ma in recent years (Smithies et al., 2018; Wyman, 2019; Lowrey et al., 2020). Taken together with numerous studies that support subduction processes in the eastern Yilgarn, the most recent evidence from the western Yilgarn implies that the ~2700 Ma plume must have ascended between two opposing and at least partially contemporaneous subduction zones. This observation carries several major implications and one of them is that the Late Archean Yilgarn plume was probably much smaller than suggested by the classic models. Although it might be argued that these constraints still allow for a Yilgarn plume tail scenario, the Archean CMB plume model is strongly tied to the purported dimensions of a Yilgarn plume head.

Abitibi Plume Dimensions

One of the few other areas that might provide an indication of Archean plume size is the Abitibi greenstone belt of the Wawa-Abitibi terrane. Dostal and Mueller (2013) assessed the size of the 2724–2722 Ma Stoughton-Roquemaure Group (SRG),

which represents early plume magmatism following its eruption through the Hunter Mine arc caldera (Dostal and Mueller, 1997; Mueller et al., 2009). Based on the extent of the komatiites and komatiitic basalts of the SRG, Dostal and Mueller (2013) argued that in its earliest stages, the Abitibi plume had a minimum diameter of ~70 km. Mapping the extent of the two subsequent main Abitibi komatiite events at 2717–21714 Ma and 2708–2704 Ma suggested the lateral extent of the plume grew to about 250 km (**Figure 1**). As also argued by Wyman et al. (2002), the hypothesized setting involves only one plume and subduction step-back in the vicinity of the Abitibi belt. Although the distribution of komatiites provides only an indication of plume extent, Dostal and Mueller (2013) considered these dimensions to be a good approximation of the final plume size. Rather than assessing the age and distribution of subsequent felsic magmatism, they considered the small-scale compositional heterogeneity within the SRG eruptions and other Abitibi komatiite-bearing sequences. Given the juvenile nature of the Abitibi arc at 2724 Ma, and the fact that main "granite bloom" did not occur until after 2700 Ma (Corfu, 1993), invocation of a Yilgarn-style variably thick lithosphere and crust is implausible as a control on the nature of plume eruptions. Instead, an alternative explanation was invoked to account for the multiple magma types found in the SRG. The authors cite the numerical modeling by Farnetani et al. (2002), which assessed thermo-chemical plumes rather than homogeneous thermal plumes. That paper showed that the heterogeneities within plume-related volcanic sequences may be linked to compositional variations, a few km-thick, originating within the starting plume itself rather than via the incorporation of large amounts of upper mantle. Dostal and Mueller (2013) considered the small-scale compositional variations found in plume-related volcanic sequences of the Abitibi belt (and elsewhere) to be consistent with the melting of filaments on a scale of 10's to 100's of m developed by stretching and folding of heterogeneities within a small plume. The proposed smaller Abitibi plume of Dostal and Mueller (2013) is more consistent with shallow mantle origins (e.g., Davies, 1995) than a classic large CMB plume, although the authors did not discuss plume sources in any detail. They also rejected the idea of multiple (CMB) plumes as implausible. This alternative would imply that, after a 100 m.y. or longer absence from the Superior Province, one plume arrived to cut through an existing arc at 2722 Ma, another at 2717–2714 Ma to overlay slightly younger arc assemblages and a third ascended to produce komatiites between 2708 and 2704 Ma and partly coincided with calc-alkaline volcanism.

Relative Timing of Mid- to Late-Archean Plumes

Associations of plume- and subduction-style magmas are often considered the product of crustal contamination of plume magmas or as evidence that plumes and associated oceanic plateaus might induce early forms of mobile lid geodyanamics (Nair and Chacko, 2008; Barnes and Van Kranendonk, 2014; Stern and Gerya, 2018). Mantle plume events might also be interpreted as the initiators of volcanic cycles when it
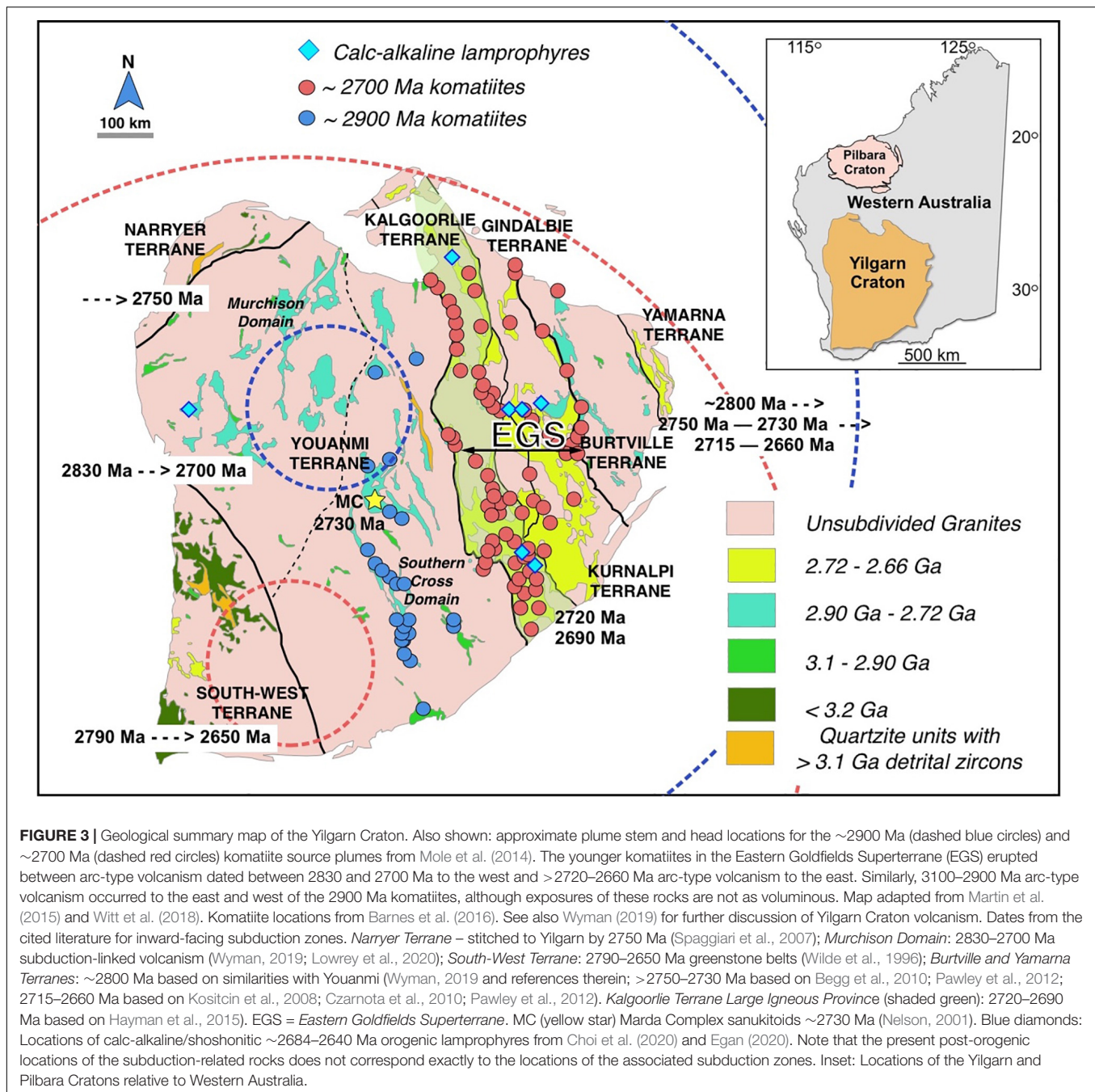
FIGURE 3 | Geological summary map of the Yilgarn Craton. Also shown: approximate plume stem and head locations for the ~2900 Ma (dashed blue circles) and ~2700 Ma (dashed red circles) komatiite source plumes from Mole et al. (2014). The younger komatiites in the Eastern Goldfields Superterrane (EGS) erupted between arc-type volcanism dated between 2830 and 2700 Ma to the west and >2720–2660 Ma arc-type volcanism to the east. Similarly, 3100–2900 Ma arc-type volcanism occurred to the east and west of the 2900 Ma komatiites, although exposures of these rocks are not as voluminous. Map adapted from Martin et al. (2015) and Witt et al. (2018). Komatiite locations from Barnes et al. (2016). See also Wyman (2019) for further discussion of Yilgarn Craton volcanism. Dates from the cited literature for inward-facing subduction zones. *Narryer Terrane* – stitched to Yilgarn by 2750 Ma (Spaggiari et al., 2007); *Murchison Domain*: 2830–2700 Ma subduction-linked volcanism (Wyman, 2019; Lowrey et al., 2020); *South-West Terrane*: 2790–2650 Ma greenstone belts (Wilde et al., 1996); *Burtville and Yamarna Terranes*: ~2800 Ma based on similarities with Youanmi (Wyman, 2019 and references therein; >2750–2730 Ma based on Begg et al., 2010; Pawley et al., 2012; 2715–2660 Ma based on Kositcin et al., 2008; Czarnota et al., 2010; Pawley et al., 2012). *Kalgoorlie Terrane Large Igneous Provinc*e (shaded green): 2720–2690 Ma based on Hayman et al., 2015). EGS = *Eastern Goldfields Superterrane*. MC (yellow star) Marda Complex sanukitoids ~2730 Ma (Nelson, 2001). Blue diamonds: Locations of calc-alkaline/shoshonitic ~2684–2640 Ma orogenic lamprophyres from Choi et al. (2020) and Egan (2020). Note that the present post-orogenic locations of the subduction-related rocks does not correspond exactly to the locations of the associated subduction zones. Inset: Locations of the Yilgarn and Pilbara Cratons relative to Western Australia.

can be shown that they erupted through significantly older cratonic crust. If big wedge tectonics apply to komatiite-forming plumes, then this apparent scenario should actually be reversed when assessed in a larger temporal and spatial context. The previously cited recent studies of the western Yilgarn demonstrate that the well-known komatiites of the Eastern Goldfields did in fact postdate subduction tectonics and the distribution of those komatiites follows a rifting event that was oriented broadly parallel to the two opposing trenches. If the Eastern Goldfield komatiite magmatism was studied in isolation, it might be concluded that a random plume head

event had again fortuitously occurred near the center of the craton. In fact, the timing and location of the Eastern Goldfield events relative to earlier and contemporary arc-style volcanism that included boninites, calc-alkaline andesitic centers, and sanukitoids (e.g., Czarnota et al., 2010; Wyman, 2019) provides an indication of the scales that are most appropriate for assessing Archean geodynamics.

The 2.7 Ga event was actually the second time that a mantle plume had arisen beneath the Yilgarn Craton in ~200 m.y. The possible relationships of the earlier ~2.9 Ga komatiites to subduction are less well preserved but they are distributed

in a similar orientation to that of their ∼2.7 Ga counterparts (**Figure 3**; Barnes et al., 2016). There is also a record of ∼3–2.9 Ga volcanism preserved in the craton, including the andesite-dacite host rocks of the Golden Grove area in the west (Whitford and Ashley, 1992; Wang et al., 1998). Dacitic volcanic rocks of this age range also occur in the eastern Yilgarn and as basement in the Kalgoorlie terrane (Pawley et al., 2012). When considered at a time scale of 10's of m.y., it becomes clear that plumes twice followed subduction in the Yilgarn. Accordingly, the craton provides evidence of two small mantle plumes ascending within "cradles" of earlier and contemporary arc-style volcanism. These relationships suggest that inward facing double subduction contributed to focused input of oceanic crust into the sub-Yilgarn MTZ while the opposing arcs induced extension with the craton itself, providing suitable pathways for the ascent of komatiitic magmas from MTZ plumes.

Wyman (2018) reviewed the case of late Archean komatiites in the Abitibi-Wawa subprovince of the Superior Province. The Abitibi plume erupted along the margin of an already assembling Superior Province Craton (Wyman et al., 2002; Percival et al., 2012). It is first observed near the top of the ∼2750–2735 Ma Pacaud Assemblage where komatiitic units overly tholeiitic and calc alkaline sequences and as eruptions of basaltic komatiites though the 2730 Ma Hunter Mine Group oceanic arc (Dostal and Mueller, 1997; Ayer et al., 2002). In a broader context, the older terranes of the Superior Province had already begun to develop renewed volcanism 10's of m.y. earlier in response to plate motions that would lead to their amalgamation in a sequence of seven or more orogenies between 2720 and 2680 Ma (Percival et al., 2012). The amount of oceanic crust consumed in the lead up to these collisions is presently impossible to quantify but the orogens themselves are well documented by structural, sedimentological and volcanological studies, igneous geochemistry, U-Pb geochronological data for igneous and xenocrystic zircons, plus deep seismic and magnetotelluric data (Percival et al., 2012). Given the number of orogens and the quick succession of accretionary events, they likely resembled the accretion of the Cimmerian terranes to Europe (Stampfli and Borel, 2002) more than the collision of India with Asia. Nonetheless, the injection of multiple slabs into the sub-Superior from the (present-day) south, north and east provided an ideal setting for big wedge processes to occur.

Cratonization – Thermal Imprints and Keel Development

Since Campbell and Hill (1988), estimates of the thermal impact of large CMB plumes on cratons and field observations have been combined to validate deep plume models and improve understanding of the cratonization process. For the Yilgarn, there is a long history of conflicting interpretations for specific features, such as the origins of individual granite suites or the spatial and temporal extent of plume-generated volcanism (Cassidy et al., 1991; Hill et al., 1992). With recognition that the 2.7 Ga Yilgarn plume head was much smaller than originally envisioned, a larger role for late Archean plate tectonic events can be considered. There are intrinsic difficulties in tracing the heat source for

granite rocks and space does not allow a full assessment of all of the features that have been ascribed to the thermal impact of the younger ∼2000 km plume head beneath the Yilgarn or the rarity of granite suites or inherited zircons that might be attributed to the older plume. Instead, we consider calc alkaline (or shoshonitic) lamprophyres to provide an alternative means of assessing the impact of a sub-cratonic flattened plume head. These types of lamprophyres include some Archean examples that have high MgO and Ni contents combined with strongly enriched incompatible element abundances that ensure their subduction-style geochemical signatures are not the product of crustal contamination. They have occurred in late orogenic settings since the Archean, commonly in association high-K intrusive rocks (e.g., syenites) and in proximity to orogenic Au districts (Wyman and Kerrich, 1988; Kerrich and Wyman, 1990). Some Archean examples in the southern Superior Province carry pyroxenite xenoliths typical of Phanerozoic sub-arc mantle suites and the xenoliths themselves display classic subduction-style trace element patterns (Wyman et al., 2015).

Choi et al. (2020) have most recently reported on calc alkaline lamprophyres of the Yilgarn craton and provided radiogenic isotope data for number of samples. In the eastern Yilgarn, these lamprophyres have emplacement ages between ∼2684 and 2640 Ma. Although the lamprophyres display strong enrichment in terms of Th/Yb signatures, Choi et al. (2020) report that they have juvenile εNd$_i$ values averaging + 0.9. The result is consistent with enrichment from juvenile arc sources along the eastern margin of the Yilgarn rather than via assimilation of older Yilgarn crust during magma ascent. This data demonstrates that prolonged thermal perturbation of the sub-Yilgarn craton linked to ∼2720–2690 Ma komatiite volcanism (Hayman et al., 2015) was unlikely, given that millions of years of subduction prior to ∼2684 Ma would typically be expected before a suitably hydrated lamprophyre source could be developed. In summary, this evidence suggests that granite rocks of the Eastern Goldfields and elsewhere in the Yilgarn are almost certainly not the product of CMB mantle plume heads re-working the existing craton.

Archean deep mantle plumes have also been widely held to be responsible for the development of buoyant refractory keels following the extraction of komatiitic volcanic suites (e.g., Herzberg, 1993, 1999). Wyman and Kerrich (2002) accepted the theory of a link between mantle plumes and keels but, like Griffin et al. (2003), they recognized that the model had problems. They cited geochronological evidence for late keel formation (or at least docking) relative to the crustal evolution of the Kaapvaal and Slave Cratons and the fact that plume ascent in the Abitibi belt was followed by shallow mantle arc and back-arc style magmatism and the development of subduction-related orogenic gold deposits, all of which precluded the presence of a refractory plume-generated cratonic keel. Additionally, the shallowest lithospheric mantle in the Superior Province underlies the southern margin where late Archean komatiite magmatism developed (Wyman, 2018), which is counter to the expectation of a link between plumes, komatiites and deep keels. Griffin et al. (2003) noted that the shallowest parts of cratonic keels resembled "modern" lithosphere derived from subduction processes, consistent with the arc-style pyroxenite xenoliths

contained in southern Superior Province orogenic lamprophyres. In the case of the Abitibi-Wawa region, Wyman and Kerrich (2002) proposed delayed ascent of the plume melt residue due to insertion of the slab associated with the Pontiac subprovince, while Griffin et al. (2003) suggested that mantle overturns or superplumes may have developed "lifebuoys" of depleted mantle that later coupled to otherwise impermanent cratons, thereby saving them from destruction.

Other examples of delayed crust-root coupling continue to be reported, such as the North Atlantic Craton and the Sask Craton in Canada (Wittig et al., 2010; Czas et al., 2020). The big wedge model for Archean plumes does not necessarily rule out the possibility that subducted slabs obstructed keel ascent beneath some cratons or that mantle overturn events independently generated "lifebuoy" keels after late Archean greenstone belts underwent crustal-level orogenic processes. The model may, however, allow for other explanations. In the ~2700 Ma Yilgarn or Abitibi, for example, the plumes may have been elongate features oriented parallel to the associated subduction zones. Only detailed future modeling can establish whether, in these more sheet- or curtain-like structures, the ascent of buoyant mantle melt residues was delayed or disrupted until orogeny eliminated the effects of wedge-related mantle convection.

KOMATIITES THROUGH TIME

If the basalt barrier – big wedge scenario was a key component of the geodynamic setting for Late Archean komatiites, then it could be argued that these processes should have made a contribution to the generation of komatiites further back in time and more recently than ~2700 Ma. In this section, three additional cases are examined. The Paleoproterozoic Circum-Superior belt is considered first because its broad geodynamic context is understood quite well (e.g., Corrigan et al., 2009) and it developed in what has been predicted to be the closing stages of a viable basalt barrier (Davies, 2008). The East Pilbara is then examined as an example of early komatiitic magmatism that is widely considered to be the product of multiple mantle plumes. Finally, the komatiites of Gorgona Island are considered, given that they are the youngest known occurrence of komatiites and post-date any basalt barrier by more than 1000 m.y.

The Circum-Superior Belt

Davies (2008) models suggest that the decline in Earth's radioactive heat generation gradually led to a cooler mantle and subducted plates that were thick and heavy enough to penetrate and disrupt the basalt barrier. As a result, the models indicate that after about 1.8–1.6 Ga there was no further mantle layering. Big wedge and basalt barrier scenarios up to that point, however, could have played a significant role in developing early Proterozoic mobile belts. The basalt barrier and an early example of the plate tectonic Wilson Cycle (Corrigan et al., 2009) should have co-existed during the 2070 M–1800 Ma life of the Manikewan Ocean that terminated with the Trans-Hudson orogen. Although the Trans Hudson has been referred to as a "proto-type of a modern orogen" (Corrigan et al., 2009), it was

preceded by the eruption of Winnipegosis komatiites and other plume-style magmas of the Circum-Superior Belt that potentially indicated interaction between mantle plume and subduction processes (Waterton et al., 2017). A 2.0 Ga Minto-Povungnituk Large Igneous Province, also occurs in the Cape Smith Belt and has been linked to a variety of other approximately co-magmatic events in the craton (Kastek et al., 2018).

Ciborowski et al. (2017) considered the preserved remnants of the Circum-Superior Belt (CSB) to be a Large Igneous Province that encircled the Archean Superior Province Craton (**Figure 4A**). From south of Lake Superior, these remnants occur in the Marquette Range Supergroup and, proceeding in a clockwise direction, include the Gunflint Formation, Thompson Nickle Belt, Fox River Belt, Sutton Inlier, Belcher Islands and other Hudson Bay islands, the Cape Smith Belt and the Labrador Trough. Prominent sets of dikes, such as the ~1880 Ma Molsen mafic dykes, along with carbonitites and lamprophyres are considered to be genetically related to the circum-cratonic magmatism.

The CSB been the subject of multiple genetic models due its unusual combination of features and its association with large-scale plate tectonic events leading up to the formation of the Nuna supercontinent. Corrigan et al. (2009) discussed the belt in the context of these accretionary events leading to the Trans-Hudson Orogen. They noted that some prior interpretations of the CSB have invoked plume interaction with the cratonic margin but argued for an "active geodynamic setting" based on the presence of older and coeval calc-alkaline magmatism along that margin. Given that the Superior Province acted as the lower plate in the later Trans-Hudson Orogen (Weller and St-Onge, 2017), it is difficult to discount the possibility that calc-alkaline counterparts to the Thompson Nickel Belt have been lost elsewhere along the boundary zone. Heaman et al. (2009) undertook a geochemical and U-Pb geochronological study of the dykes, sills and volcanic rocks that comprise the "Molsen Igneous Events" in the Fox Lake and Thompson Nickel belts of northern Manitoba. They found that most of the rocks fell within a narrow 8 million-year age range between 1885 and 1877 Ma. In assessing the setting of the magmatism, they noted arguments against a plume including lack of a radiating dyke swarm or cratonic uplift, the absence of Ocean Island Basalt-type magmas and the widely dispersed nature of the volcanism. They favored "an unusual tectonic setting that has no modern or ancient analog" (p. 160). Other workers, such as Ciborowski et al. (2017) and Bleeker and Kamo (2018) remain in favor a mantle plume scenario with the latter stating " we interpret the overall geodynamic setting in terms of a hot mantle upwelling, possibly a deep-seated mantle plume, that impinged on the base of Superior Craton's subcontinental lithosphere (p. 10)."

In the context of the MTZ model of komatiite generation, Heaman et al.'s (2009) description of a unique CSB event with neither older or younger analogs is notable, given that the time in question combines Himalayan-scale accretionary processes (Weller and St-Onge, 2017) and a "prototype modern orogen" with the proposed last stages of an effective basalt barrier. Although the Superior Craton acted as the lower plate in the Trans-Hudson orogen, its margins were associated with a range
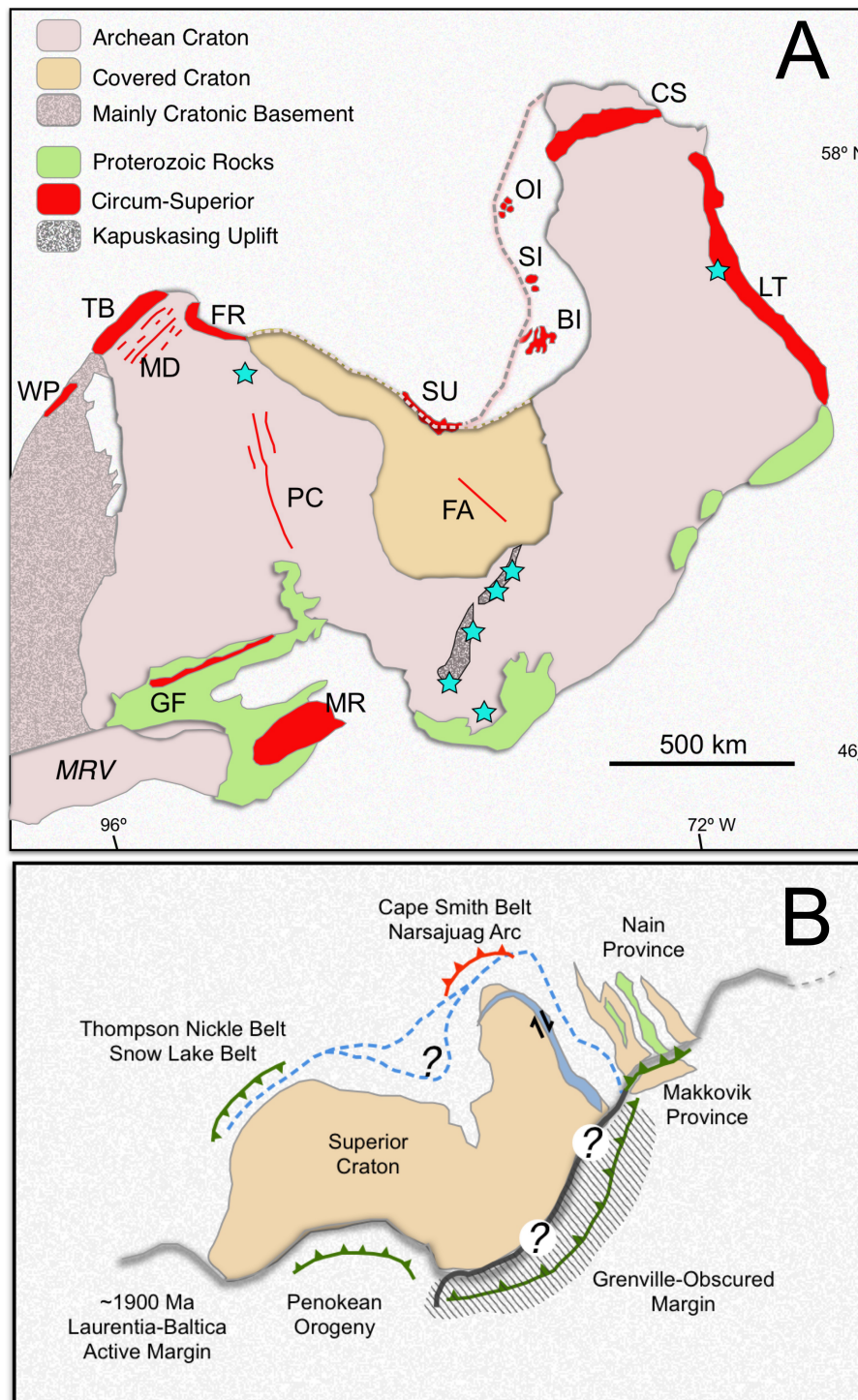
FIGURE 4 | (A) Map of the Superior Craton and ~1885–1864 Ma Circum-Superior Belt. Red lines: ~ coeval dikes; blue stars: ~1885–1864 carbonitites. Dashed gray line: possible deep crustal extension of cratonic margin (see: Corrigan et al., 2009). MRV, Minnesota River Valley Terrane. Map adapted from Ciborowski et al. (2017) with modifications from Percival et al. (2012) and Waterton et al. (2017). ~1885–1864 Ma mafic magmatism: BI, Belcher Islands; CS, Cape Smith Belt; FA, Fort Albany dykes; FR, Fox River Belt; GF, Gunflint Formation; LT, Labrador Trough; MR, Marquette Range Supergroup; MD, Molson dykes; OI, Ottawa Islands; PC, Pickle Crow dyke; SI, Sleeper Islands; SU, Sutton Inlier; TB, Thompson Nickel Belt; WP, Winnipegosis Belt. **(B)** Convergent margin processes around the Superior Province Craton at ~1900 Ma. Blue dashed lines indicate possible locations of the Superior Craton margins at ~1.9 Ga (Corrigan et al., 2009). Given the co-temporal flips to craton-facing subduction in the Penokean Orogeny and the Makkovik Province, a similar flip may have occurred all along the southern Superior Craton. Simplified from Ketchum et al. (2002), with additions from sources for map in panel **(A)**, and St-Onge et al. (2006) and Schulz and Cannon (2007).

of geodynamic events a few million years prior to, and around the time of, eruption of the Winnipegosis Komatiites.

The large-scale geodynamic context of the CSB starts with the Manikewan Ocean. It had reached its maximum extent by 1920 Ma and was contracting as Archean cratonic blocks and intra-oceanic arcs accreted to the west and north in the Western Churchill Province and the Reindeer Zone respectively (e.g., Ansdell, 2005). On the other side of the ocean, emplacement of calc-alkaline plutons dated back to at least 1891 Ma in the Thompson Nickel Belt (Percival et al., 2005), CSB magmatism was coeval with calc alkaline magmatism in the Snow Lake belt and Cape Smith Belt magmatism overlapped that of the Parent Arc (Corrigan et al., 2009). Along the south west embayment of the Superior margin, the circa 1880 Ma collision of the Pembine-Wausau terrane at the onset of the Penokean Orogeny was associated with a flip to craton-facing subduction (**Figure 4B**; Schulz and Cannon, 2007). Events further to the north-east along the Superior Craton margin are now obscured by the Grenville orogen. The Penokean Orogen, however, was part of the extensive Laurentia-Baltica active margin that reemerges in Labrador and then continues further east into Greenland and Karelia (Ketchum et al., 2002). The collision of the Paleoproterozoic Makkovik Province with the composite Nain Craton is preserved in Labrador following a switch to craton-facing subduction sometime between 1895 and 1870 Ma (Ketchum et al., 2002). Meanwhile, within the Superior Province, the Kapuskasing Uplift Zone developed at circa 1900 Ma in what is widely considered to be a response to stresses applied to the margins of the Superior Province Craton (e.g., Perry et al., 2006). Evans and Halls (2010) undertook a study to establish the Superior Province configuration prior to the uplift that, based on the geochronological evidence they summarized, mainly occurred at 1880 Ma. They considered whether the uplift might have been solely related to the contemporary and nearby Penokean Orogeny but discounted this possibility on the basis of the soft Penokean collision inferred by Schulz and Cannon (2007). They preferred a scenario where other plate-boundary forces drove the western Superior Craton southward relative to the eastern section, but conceded it remains difficult to test such a model.

Based on the summary of circum-Superior events presented here, and the numerous uncertainties involved, only a broad application of the basalt barrier – big wedge model is possible. The available evidence suggests that the most significant large-scale geodynamic change around the time was a switch from encirclement by converging, outward-facing, subduction zones in the Manikewan and pre-Penokean Oceans to the near-simultaneous development of craton-facing subduction in the western Superior and perhaps around the majority of the craton. As a result, a scenario resembling the ~2700 Ma Yilgarn Craton would have been created in at least the western Superior and perhaps more widely. A plume originating in the MTZ could develop in response to the changed geodynamic conditions whereas involvement of a CMB plume, if that was even feasible at this time, would be highly coincidental. Once again, a CMB plume would be required to ascend between subducting slabs. The north-facing subduction was terminated

by 1850 Ma when the Marshfield Terrane accreted to the Pembine-Wausau Terrane along the southern Superior margin leading to development of the Penokean fold and thrust belt (Schulz and Cannon, 2007).

A basalt barrier model allows for resolution of many of the key issues invoked in support of both a convergent margin setting and contemporary plume magmatism and provides another example of how komatiites were associated with inward-facing subduction zones. The lack of a classic set of radiating dikes may signify that the upwellings did not form a flattened mushroom-shaped head but instead took the form of irregular sheets consisting of warmed and displaced transition zone mantle (±contributions from the region just below the 660 km boundary). Thrusting and crustal uplift along the Kapuskasing Zone would be a consequence of plate tectonic events along the margins of the Superior Province craton but a short-lived thermal anomaly beneath the region may have been associated with the MTZ plume or other big wedge processes that provide smaller scale thermal anomalies (e.g., **Figure 2**; Geng et al., 2019). In the basalt barrier – big wedge scenario, the carbonitites shown in **Figure 4A** are not required to originate in the plume but could instead be a manifestation of large-scale production of carbonatic melts from the subducted slab itself (Li et al., 2017). In summary, the basalt barrier – big wedge model provides a unique way to resolve the main controversies associated with the Circum-Superior Belt while also highlighting features such as the association of inward-facing double subduction zones and komatiitic magmatism that it shares in common with the Yilgarn Craton.

The Pilbara Puzzle
A Problematic Model

The East Pilbara Craton is the archetypal early Archean craton and is widely accepted to have been derived from, or modified by, mantle plumes in its earliest preserved stages. Satellite images of the craton display no features that demand plate tectonics, lending credence to this scenario. It has been suggested that eight ~15 m.y. (ultra)mafic to felsic cycles represent repeated plume events in the 3530–3230 Ma Pilbara Supergroup, which were punctuated by 75 and 60 m.y gaps in volcanism between the Warrawoona, Kelly and Sulphur Spring Groups (Van Kranendonk et al., 2007; Hickman and Van Kranendonk, 2012). The model challenges what is known about plumes based on the geological record. In fact, a paper by Van Kranendonk et al. (2002) includes a statement that, at that time, only two of its five authors favored nearly continuous mantle melting beneath the East Pilbara that *may* have been attributed to recurrent mantle plumes. Wyman (2013) also considered the eight-plume model to present a Pilbara dilemma. Why did so many plumes find the small Pilbara craton in quick succession? Was the Pilbara typical of the crust at that time but unique in its preservation of a massive global mantle plume event? Could globe-covering plume events exist, given that plumes are defined by their anomalous temperatures relative to the upper mantle? Mantle overturns, as commonly envisioned, do not suggest such pulses of plume events, global or otherwise. In any case, if the big wedge model is to be considered viable, then it should probably apply to the early

Archean Pilbara as well as the Late Archean and Paleoproterozoic cases discussed up to this point.
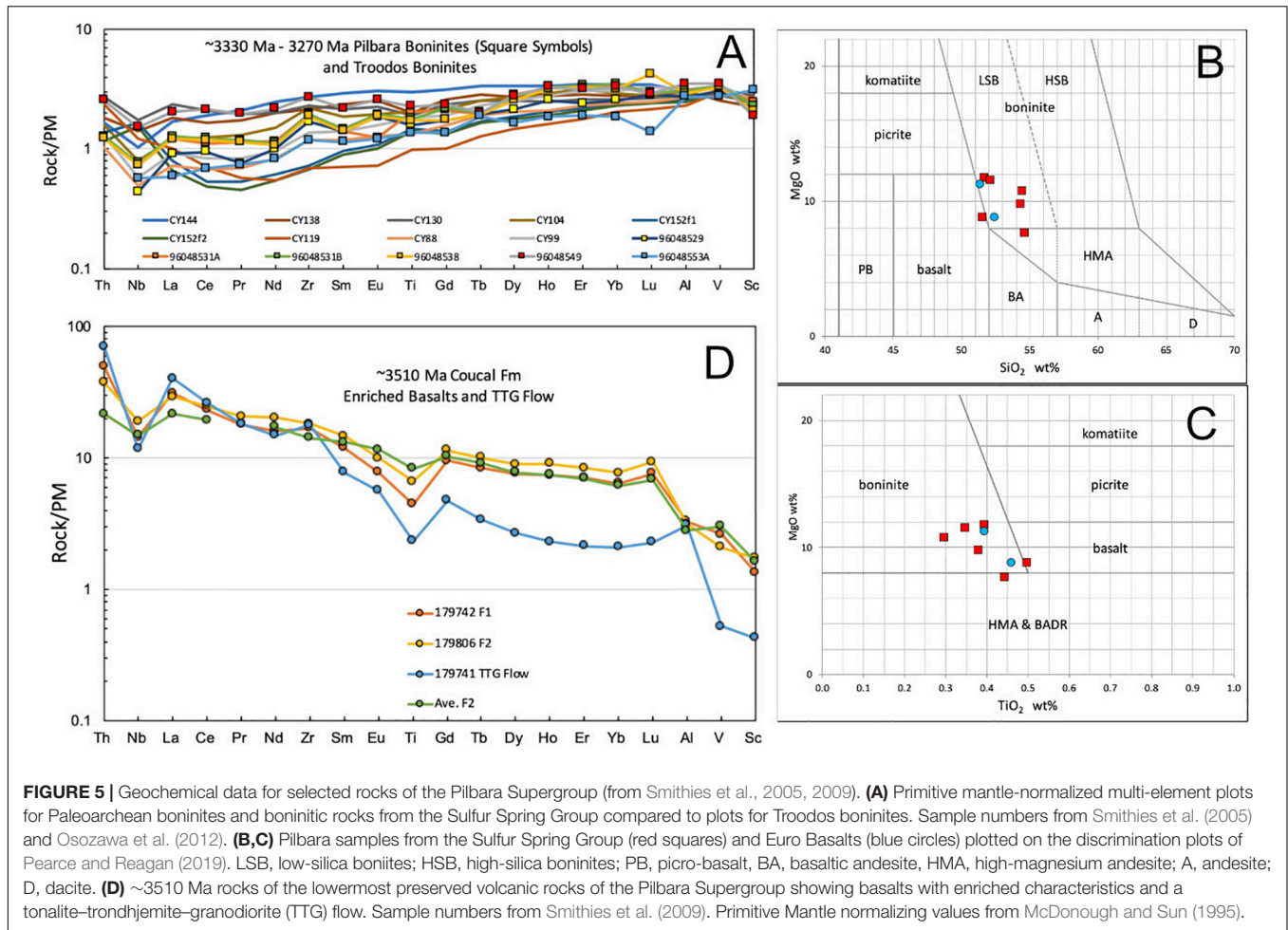
A Case of Mistaken Identity

One possible explanation to the challenge presented by the Pilbara multi-plume model is that one or more of the underlying observations or interpretations is incorrect. The eight plume events are actually defined only by basaltic rocks and not true komatiites. If some of these basaltic units were not related to mantle plumes, then a very different scenario is possible. Technically, basaltic rocks should only be labeled as komatiitic basalts if they can be shown to have a genetic relationship to true komatiites (Arndt et al., 2008). These rocks commonly display pyroxene spinifex textures, which are the "principle diagnostic feature of komatiitic basalt" (Arndt et al., 2008, p. 93). For pyroxene spinifex to be uniquely associated with "komatiitic basalt," however, it would need to be closely related to some feature of komatiite composition or its thermal history, perhaps including earlier magma superheating, for example.

Several lines of evidence suggest that pyroxene spinifex textures, as found in komatiitic basalts, are not exclusively a function of magma composition but also of some other factors. Experimental studies to understand pyroxene spinifex formation lacked reproducibility (Bouquain et al., 2014), which is consistent with this possibility. Field observations from non-Pilbara localities are of relevance to the pyroxene spinifex issue. Like the Pilbara Supergroup, evidence for shallow marine environments based on stromatolites are common in the Archean Nondweni greenstone belt (Wilson et al., 1989; Wilson and Versfeld, 1994) and in the Paleoproterozoic Hekpoort Formation of the Transvaal sub-basin (Humbert et al., 2018). Given the occurrence of pyroxene spinifex across a wide range of compositions extending to andesites, Wilson et al. (1989) inferred that the shallow marine setting was responsible for the formation of pyroxene structures in the Nondweni lavas, including the meter-scale aggregates of giant spinifex. Wilson and Versfeld (1994) inferred that loss of steam in shallow water conditions was a key factor in the cooling history of these lavas. Such settings were common in Archean and Paleoproterozoic cratons. The presence of both pyroxene spinifex and basin-localized varioles in the Hekpoort formation was also suggested by Humbert et al. (2018) to be related to undercooling of lavas with typical MgO contents in the 5–8 wt% range. In the Youanmi Terrane of the western Yilgarn, pyroxene spinifex textures are also reported in flows with MgO contents as low as 5.6 wt% MgO (Van Kranendonk et al., 2013; Lowrey et al., 2017). It seems implausible that a parental komatiite magma, with perhaps 25 wt% MgO, passed on some unique "spinifex trait" to magma that evolved to 6 wt% MgO. Rocks from multiple western Yilgarn volcanic series display acicular to skeletal pyroxenes, which is likely the reason that boninites and boninite-like rocks (depending on the sample and classification system: Lowrey et al., 2020) were not recognized until reported by Wyman and Kerrich (2012).

Other aspects of the Pilbara geodynamic model also require careful assessment. Smithies et al. (2005) investigated the abundant basaltic volcanism of the 3515–3240 Ma Pilbara Supergroup and demonstrated that these rocks fell into two distinct groups of Low- and High-Ti types. The High-Ti type did not vary greatly over the 300 m.y. interval and were considered to be derived from a source resembling primitive mantle. The Low-Ti examples, however, were considered to display distinct secular trends to lower incompatible element abundances consistent with increasing depletion of a single long-lived source. Smithies et al. (2005) argued convincingly that the two basalt types could not have both been derived from within ascending plumes and that the progressive depletion of the Low-Ti basalt source must have happened outside of any plumes. Having attributed some occurrences of LREE enrichment in the Low-Ti suite to local crustal contamination, they concluded that the low La/Nb and La/Yb ratios of many of the basalts indicated that any subduction or other fluxing process was of "only local" importance, which was limited by the main trends to lower La/Yb and Gd/Yb over time. On this basis, a progressively depleted lithospheric source, repeatedly melted by ascending plumes was favored for the low-Ti basalts. The trends discussed by Smithies et al. (2005), however, are only defined by the lowest La/Nb (etc) for each of the various basalt populations. If the multi-plume scenario had been independently established by other means, then the rationale for using these "least contaminated" end-member samples to define events in the Pilbara would be clear. If, however, the details of the plume scenario are not assumed *a priori*, then the putative lithospheric source of the low-Ti basalts is less certain. In fact, the most incompatible element-depleted of these volcanic units exhibit several typical features of boninitic magmas, such as $TiO_2 < 0.5$ wt%, Al_2O_3/TiO_2 between 26 and 48, depletion of the MREE vs. the HREE and positive Zr anomalies (Smithies et al., 2005; **Figure 5A**). Phanerozoic boninites exhibit diverse trace element and rare earth patterns on normalized plots. At Troodos, for example, two boninites types have long been recognized. One of these, referred to as the depleted boninites suite by Osozawa et al. (2012), displays the well-known "spoon-shaped" rare earth patterns whereas the other boninite suite does not. A comparison of the Pilbara rocks with the Troodos occurrences (**Figure 5A**) demonstrates that they have mantle-normalized patterns intermediate between the two younger suites (Osozawa et al., 2012). In addition, many of the low-Ti Sulphur Springs samples of Smithies et al. (2005) fall in the high-silica boninite field on the recent discrimination plots of Pearce and Reagan (2019), as shown in **Figures 5B,C**. On this basis, the Pilbara samples are considered here to be true boninites.

A subsequent paper by Smithies et al. (2009) argued that incompatible element enriched lowermost basaltic to andesitic rocks (**Figure 5D**) preserved in the Pilbara Supergroup (the Coucal Formation from the Coonterunah Subgroup) must be representative of large volumes of > 3500 Ma mafic rocks required to generate the 3500–3420 Ma Pilbara tonalite–trondhjemite–granodiorite (TTG) suite. Based on the preserved structural and stratigraphic evidence, the authors argued that a modern-style convergent margin setting could be ruled out during the interval preserved in the Pilbara Supergroup deposition, but they acknowledged that some sort of early form of plate subduction may have been responsible for the incompatible element enrichments in the source of the Coonterunah basalts, although some of the rocks display Nb/Zr ratios greater than primitive

FIGURE 5 | Geochemical data for selected rocks of the Pilbara Supergroup (from Smithies et al., 2005, 2009). **(A)** Primitive mantle-normalized multi-element plots for Paleoarchean boninites and boninitic rocks from the Sulfur Spring Group compared to plots for Troodos boninites. Sample numbers from Smithies et al. (2005) and Osozawa et al. (2012). **(B,C)** Pilbara samples from the Sulfur Spring Group (red squares) and Euro Basalts (blue circles) plotted on the discrimination plots of Pearce and Reagan (2019). LSB, low-silica boninites; HSB, high-silica boninites; PB, picro-basalt, BA, basaltic andesite; HMA, high-magnesium andesite; A, andesite; D, dacite. **(D)** ~3510 Ma rocks of the lowermost preserved volcanic rocks of the Pilbara Supergroup showing basalts with enriched characteristics and a tonalite–trondhjemite–granodiorite (TTG) flow. Sample numbers from Smithies et al. (2009). Primitive Mantle normalizing values from McDonough and Sun (1995).
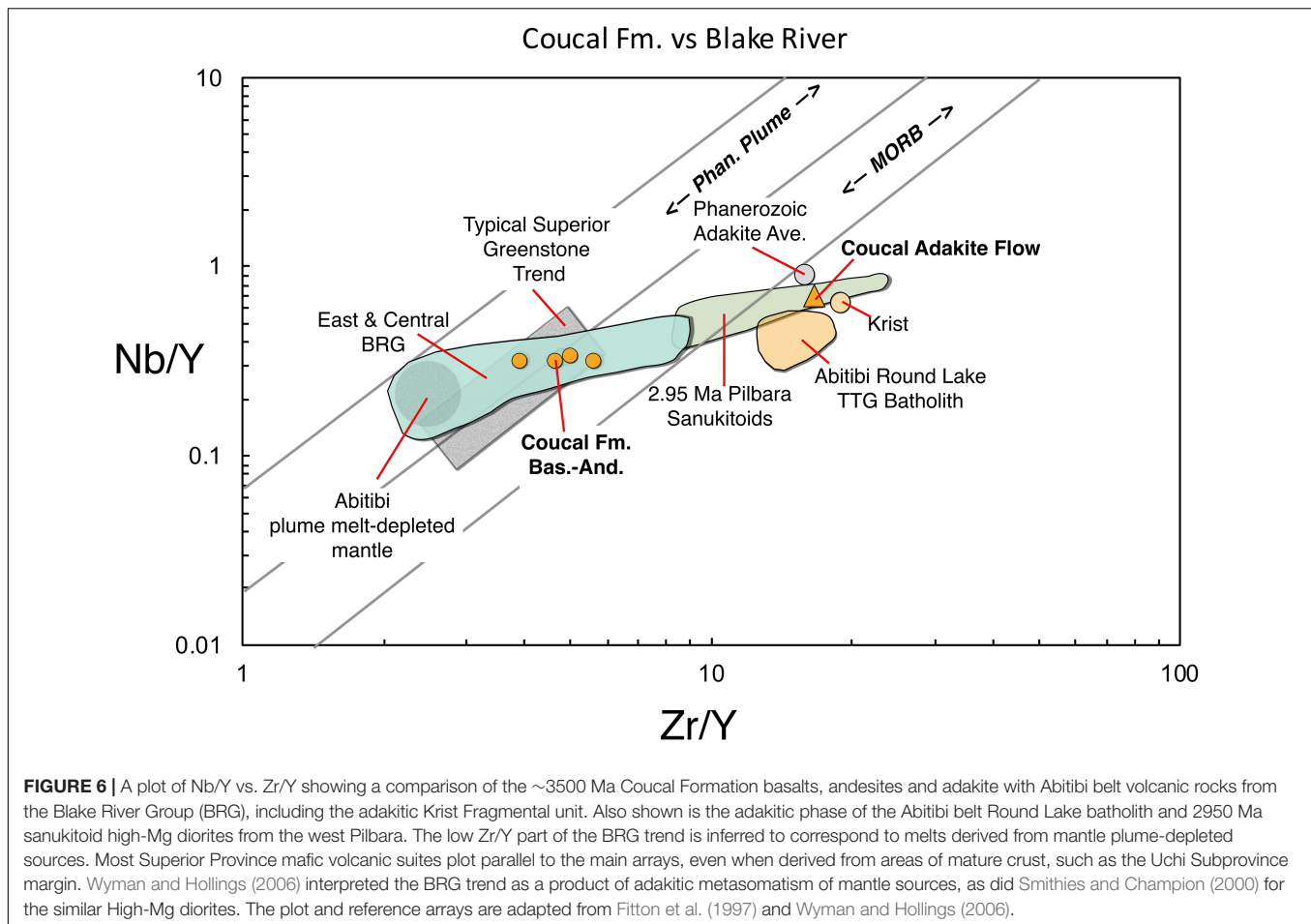
mantle. Their overall compositions and lack of contamination (Smithies et al., 2009) suggest that they are what they appear to be: products of a subduction-style process. More specifically, the enriched basalts appear similar to some units in the Abitibi Belt's Blake River Assemblage and the TTG flow is comparable to the adakitic Krist Fragmental unit, both of which erupted prior to the Abitibi's main "granite bloom" (Wyman et al., 2002). Although it is now recognized that most Archean TTG are not adakitic, the southern Superior is one of several areas where Archean adakitic plutons do occur (Smithies, 2000) and the effect of slab melts on the sources of mafic volcanism can be monitored via trends on trace element plots (Wyman, 2003). The Coucal Formation rocks directly overlap mafic Blake River Group magmas on a plot of Nb/Y vs Zr/Y (**Figure 6**) and therefore are considered here to represent a similar subduction-related suite, despite the ~800 million years separating the two sets of rocks and the strong possibility that a global set of tectonic plates did not exist at ~3500 Ma. Notably, Smithies and Champion (2000) reported on a 2.95 Ga sanukitoid High-Mg diorite suite from the west Pilbara Craton with chemical characteristics that they inferred to be derived from an adakite melt-modified mantle source. The trend of the diorites in **Figure 6** corresponds closely to both the Abitibi Blake River trend and the trend of the Coucal Formation rocks.

The Alternative Transition Zone Model

The geodynamic model defined collectively by Smithies (2002), Van Kranendonk et al. (2002, 2007), Smithies et al. (2005), Smithies et al. (2009), and Hickman and Van Kranendonk (2012) remains prominent in the literature and includes some form of subduction prior to 3530 Ma, multiple short plume cycles interspersed with several quiet intervals between 3530 and 3230 Ma and mainly Phanerozoic-style subduction processes after 3230 Ma. In a revised scenario for the 3530–3230 Ma interval, based on the MTZ source model, the presence of boninites and other subduction-style magmas can be proposed that does not contradict the lack of evidence for a "a modern-style convergent margin setting" or require a set of globe-covering tectonic plates.

As envisioned in numerical models for incipient Archean subduction, or the global onset of plate tectonics, it is possible that between 3530 and 3230 Ma the conditions required for self-sustaining subduction were being approached but the overall global regime would still be classified as episodic between stagnant and mobile lid regimes. Even when conditions for subduction initiation were present around the Pilbara Craton (**Figure 7**), the process tended to fail quickly via the loss of subducted slab (e.g., van Hunen and Moyen, 2012). The new model for the early- to mid-Archean follows on from the results

FIGURE 6 | A plot of Nb/Y vs. Zr/Y showing a comparison of the ~3500 Ma Coucal Formation basalts, andesites and adakite with Abitibi belt volcanic rocks from the Blake River Group (BRG), including the adakitic Krist Fragmental unit. Also shown is the adakitic phase of the Abitibi belt Round Lake batholith and 2950 Ma sanukitoid high-Mg diorites from the west Pilbara. The low Zr/Y part of the BRG trend is inferred to correspond to melts derived from mantle plume-depleted sources. Most Superior Province mafic volcanic suites plot parallel to the main arrays, even when derived from areas of mature crust, such as the Uchi Subprovince margin. Wyman and Hollings (2006) interpreted the BRG trend as a product of adakitic metasomatism of mantle sources, as did Smithies and Champion (2000) for the similar High-Mg diorites. The plot and reference arrays are adapted from Fitton et al. (1997) and Wyman and Hollings (2006).
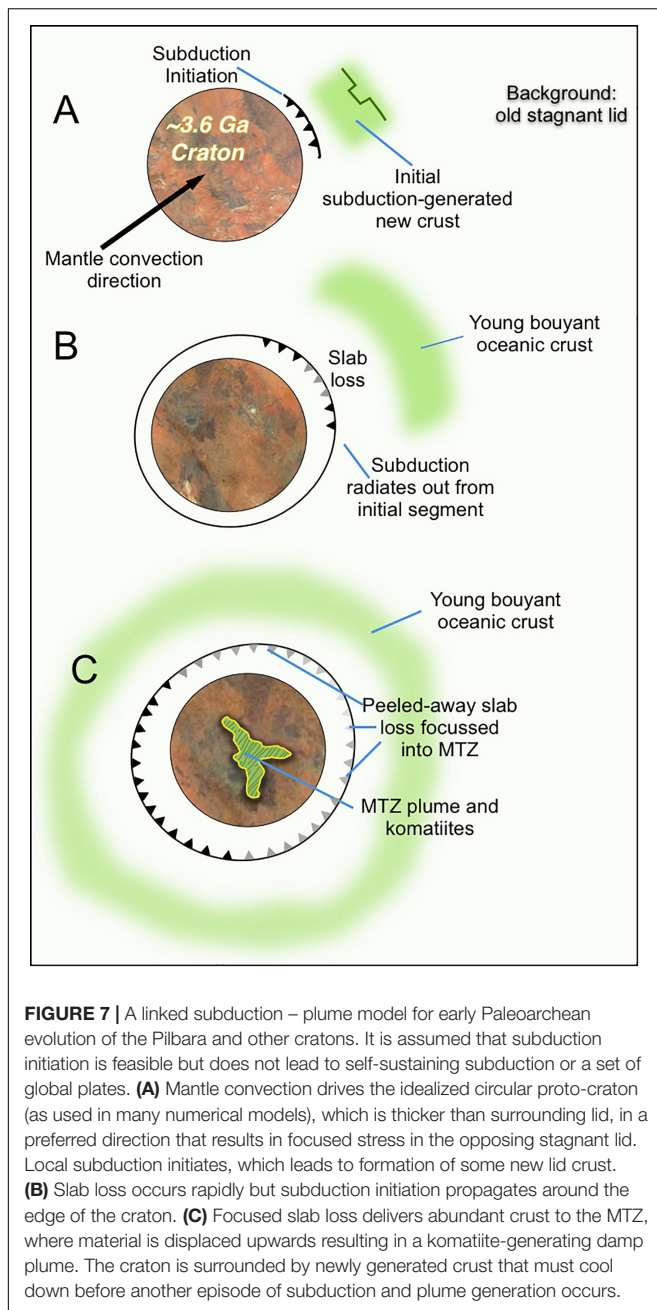
of numerical studies for subduction initiation, which envision localized stress focusing in the stagnant lid as thicker cratonic crust is forced along by mantle flow (Rolf and Tackley, 2011). In response, a subduction-like process is initiated on one side of the craton but instead of developing into a trench that extends outward from the craton to form a tectonic plate, the slab is soon lost at the initiation site, which leads to an unpeeling of similarly dense crust around the craton margin. The result is not self-sustaining subduction. Instead, a significant volume of stagnant lid crust is rapidly delivered to the sub-Pilbara MTZ and/or basalt barrier, leading to the development of a brief episode of mantle upwelling and komatiite (or komatiitic basalt) magmatism. At this point, the craton is ringed by a combination of old dense stagnant lid and younger buoyant crust generated in response to loss of stagnant lid around the craton. Once the "life buoy" of young crust has aged it no longer resists subduction initiation and another proto arc- MTZ plume sequence can develop. None of these short-lived subduction events impose a dominant structural fabric resembling a modern convergent margin.

In this model, the Pilbara and similarly aged cratons become "arc-plume circuits" that focus volcanism, plutonism and mantle heat loss but they existed in isolation (**Figure 8**) with little chance of accretion or other interaction unless their origins via mantle overturn, bolide impact, "heat pipes," etc. (see Wyman, 2018

and references therein) caused them to originally occur in close proximity. Importantly, the specific processes associated with the formation of komatiites and boninitic rocks could persist through the Archean and into the Proterozoic even as plate tectonics developed. The later evolution of the Pilbara Craton appears to have resulted in 3.2 Ga rifting that resembled the classic plate tectonic Wilson Cycle (Van Kranendonk et al., 2010). In the model suggested here, however, the change in tectonic style only requires strengthening of the subducted plate due to either (a) changing global mantle properties and their impact on the remaining stagnant lid or (b) the subduction of new crust generated by relatively recent arc-plume circuits. Once infant subduction zones could persist for extended periods, the symmetry of the early proto-cratons would have been less likely to perpetuate. In any case, the 3015 Ma "intra-cratonic" boninites of the Mallina Basin described by Smithies (2002) cannot be considered geodynamically unique in the craton's history. They relate to just one example of subduction initiation that occurred sporadically for 100's of m.y. around the small Pilbara Craton.

It should be noted that an alternative category of geodynamic model views early Archean cratons as reworked examples of typical Paleoarchean stagnant lid rather than anomalies within or on the stagnant lid. Pilbara examples include the models of Zegers and van Keken (2001) and Wiemer et al. (2018).

FIGURE 7 | A linked subduction – plume model for early Paleoarchean evolution of the Pilbara and other cratons. It is assumed that subduction initiation is feasible but does not lead to self-sustaining subduction or a set of global plates. **(A)** Mantle convection drives the idealized circular proto-craton (as used in many numerical models), which is thicker than surrounding lid, in a preferred direction that results in focused stress in the opposing stagnant lid. Local subduction initiates, which leads to formation of some new lid crust. **(B)** Slab loss occurs rapidly but subduction initiation propagates around the edge of the craton. **(C)** Focused slab loss delivers abundant crust to the MTZ, where material is displaced upwards resulting in a komatiite-generating damp plume. The craton is surrounded by newly generated crust that must cool down before another episode of subduction and plume generation occurs.

The latter cites global patterns in the generation of <3600 Ma felsic crust as evidence for the impact of peak mantle potential temperature on volcanism and the Archean proto-crust. The dome and keel map patterns of Paleoarchean cratons are commonly invoked as evidence against subduction processes (generally framed in terms of plate tectonics) and in support of intra-crustal processes that create TTG batholiths. These processes would typically have resulted in delamination of dense garnet-bearing restite, although such delamination events are also commonly associated with post-Archean terranes (e.g., Wang et al., 2007). Briefly, the reasons such models are not favored here include: they imply (nearly) global stagnant lid reworking,

resulting in a "Pilbara Earth" covered in stagnant lid-derived early craton; they do not recognize mantle overturn events (Griffin et al., 2014; Wyman, 2018), the associated thermal evolution of the mantle or the potential for some form of basalt barrier; the crustal starting material (for Wiemer et al., 2018) is the enriched basalts of Smithies et al. (2009), which resemble the basalt-andesites of the Abitibi belt's ∼2700 Ma Blake River Group and other rocks derived from slab melt-modified mantle; multiple types of mantle-derived volcanism continue through the proposed periods of intra-crustal overturn and melting and in some instances includes incompatible element-depleted boninite (-like) rocks that are widely regarded to be uncontaminated or very weakly contaminated magmas (e.g., Smithies et al., 2005 and references therein).

Gorgona Island Komatiites

As previously noted, studies of the youngest known komatiites on Gorgona Island demonstrate that they were are also derived from magmas with 0.2–1.0 wt% H_2O and display B isotope systematics consistent with derivation from fluids that originated in a subducted slab (Kamenetsky et al., 2010; Gurenko and Kamenetsky, 2011). Kamenetsky et al. (2010) also reported that initial komatiite crystallization temperature was 1330–1340°C, which is at the upper limit of temperatures recorded in mid-ocean rift basalts. Based on Sm-Nd and U-Pb data, Hauff et al. (2000) argued that basalts of the Caribbean Large Igneous Province (CLIP) was associated with rapid recycling of plume components, possibly in less than 300 m.y., depending on assumptions made about the nature of the source components. Given their depleted compositions, the Gorgona komatiites and picrites required additional source depletion within 200–300 m.y. that would be consistent with a component corresponding to the residues of MORB generation or recycled lower oceanic crust. These observations are broadly supportive of a transition zone source for the komatiites, particularly since big wedge models could supply a slight elevation of temperature within the plume without any heat contribution from the now extinct basalt barrier. But while the geodynamic context of the CLIP has been the subject of much debate for several decades, no model has invoked a shallow mantle source for the plume.

Recent key developments regarding the CLIP, as presently defined, include the fact that newer global plate reconstructions do not permit its derivation entirely from the Galapagos Hot Spot as had previously been assumed (Seton et al., 2012; Boschman et al., 2014). The uncertainties in these reconstructions increase further back in time, however, and it is more plausible or feasible that older CLIP assemblages in Costa Rico, such as the ∼178–172 Ma Nicoya Complex and the ∼125–84 Ma Manzanillo Terrane (host to the high-T Tortugal picrites described by Trela et al., 2017), did originate with the Galapagos plume (Andjić et al., 2019; Fletcher et al., 2020). This scenario would be consistent with, for example, the finding by Whattam and Stern (2015) that there were two distinct phases of magmatism associated with the LIP and that there was geochemical evidence for two oceanic plateaux in the region (Kerr and Tarney, 2005). Age determinations show CLIP volcanism extended through the Late Cretaceous (98.7 ± 7.7. Ma to 64.4 ± 5 Ma) with
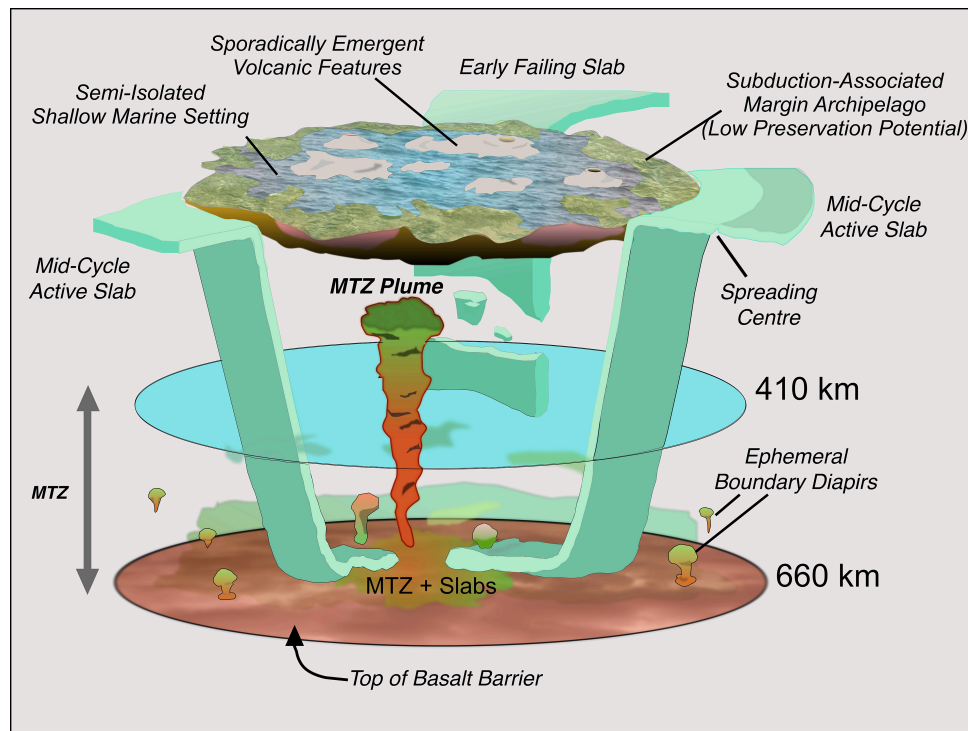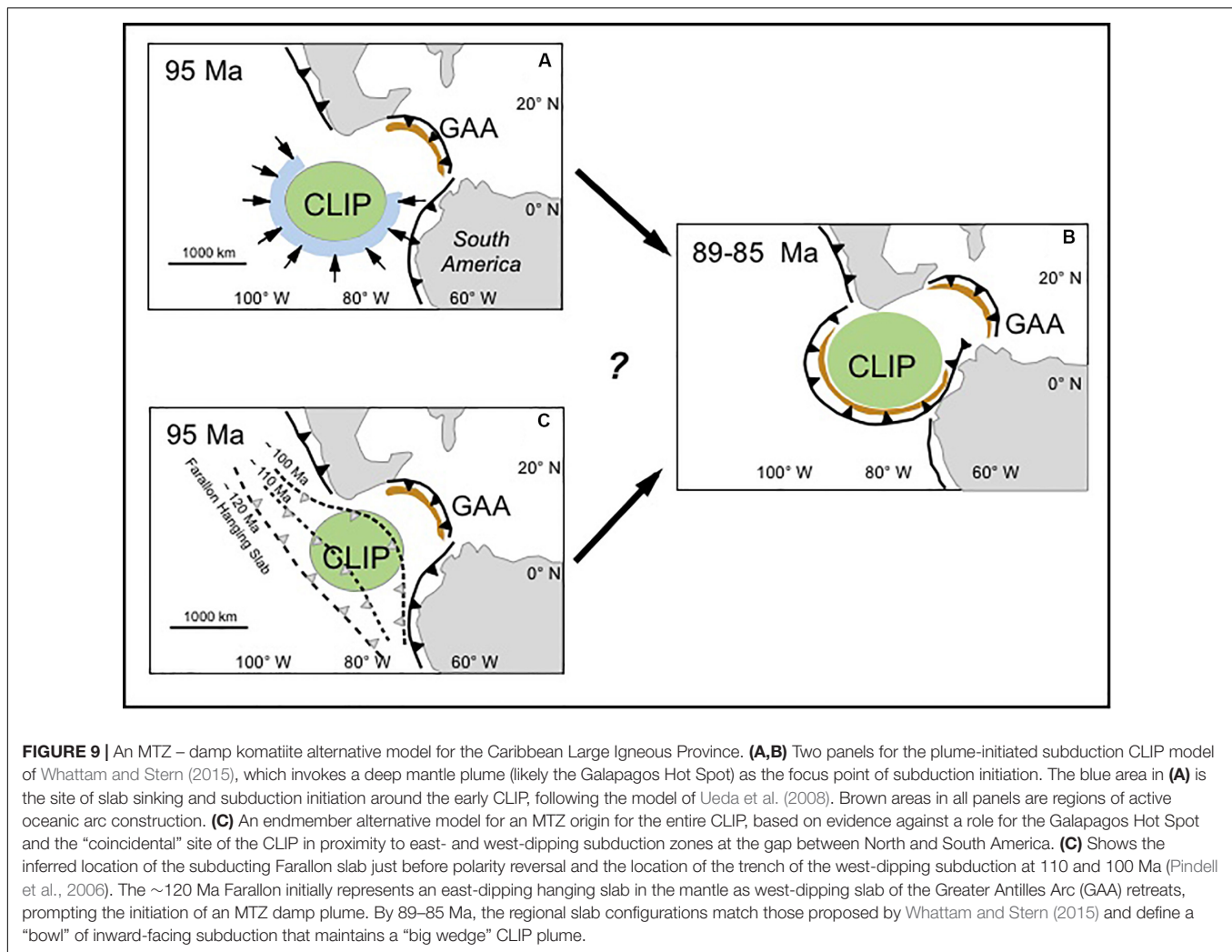
FIGURE 8 | An idealized version of the pre-plate tectonic subduction – plume circuit. Relatively small (~1000 km-scale) proto-cratons, such as the early Pilbara, focus stress in the adjacent stagnant lid and initiate subduction. Local failure of subduction occurs but the event propagates around the craton. Subducted slab accumulates in a small volume of the MTZ (above "the basalt barrier"), which displaces a mixture of mainly MTZ peridotitic mantle and lesser amounts of entrained slab crust to form a mantle plume beneath the craton. Cratonic margins may have been reworked by succeeding circuit episodes and later events. Note that the Pilbara craton's present margins are mainly obscured under cover or offshore (e.g., Hickman and Van Kranendonk, 2012). Small diapirs shown outside the region of subducting slabs reflect the fact that, as a significant thermal boundary, the basalt barrier could generate minor peridotitic upwellings anywhere. The spatial and temporal association of arc and plume volcanism in the geological record, however, demonstrates that big wedge settings facilitated the formation of plumes that were large enough to ascend through the mantle. The early cratons developed independently but global variations in mantle convection intensity may establish peak periods for circuit activity. By the late Archean, other subduction configurations were possible (e.g., inward-facing double subduction zones) and may have led to more sheet-like mantle upwellings.

komatiitic volcanism being among the youngest events (Serrano et al., 2011). Dürkefälden et al. (2019) suggested that depleted ~81 Ma magmas of the Nicaraguan Rise, located between Central America and the Greater Antilles, represent upwelling of still hot CLIP mantle in response to crustal thinning. As summarized by Whattam and Stern (2015), however, there is significant spatial and temporal overlap between plume- and arc-type lavas with no clear hiatus between them. A very wide range of geodynamic models has been proposed for the region. For the purpose of the present paper, two models are chosen for discussion.

The Whattam and Stern model (2015; see also Stern and Gerya, 2018) attempts to resolve the close association of plume and arc magmas with a plume induced subduction initiation, based on the numerical modeling of Ueda et al. (2008). The progressive additions of subduction-related contributions to the CLIP and overlapping isotopic compositions of the plume and arc magmas were considered strong evidence in favor of the model. The original plume was tentatively suggested to be the Galapagos Hotspot, but regarding the continuing plume magmatism they state "The Caribbean Plume event may have

been some sort of backarc basin magmatism associated with the Greater Antilles Arc, but it is not necessary for the plume induced subduction initiation model that the precise nature of the plume event be understood." (p. 57). Regarding the issue of why such subduction initiation events are not observed around other plateaus, Whattam and Stern (2015) raise the possibility that pre-existing subduction to the north and south may have contributed to the subduction initiation event. Nevertheless, they hold out the prospect that the model has relevance to the development of Archean cratons.
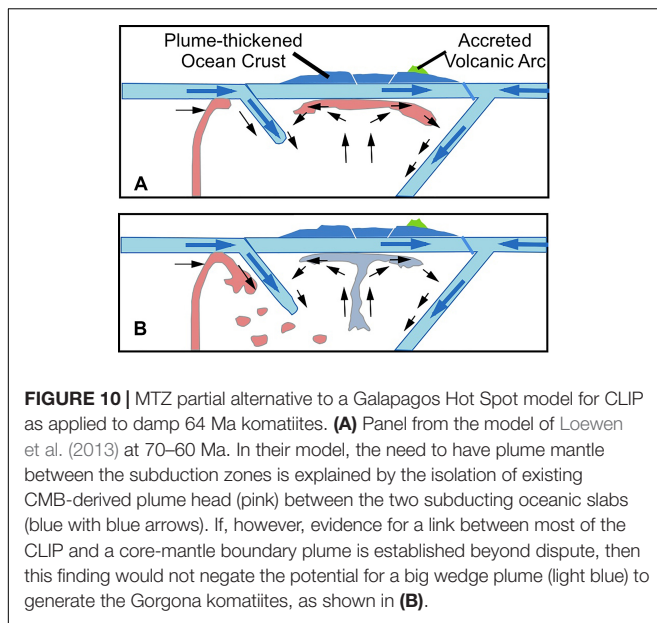
The suggestion of a possible back arc-related plume resembles the big wedge models cited as a basis for the MTZ damp komatiite model. A full-fledged MTZ plume model, however, can be presented as an endmember alternative to the Whattam and Stern (2015) model (**Figure 9**). Justifications would include: (i) the observation that in many cases (Pilbara, Yilgarn, Superior Province, Trans-Hudson) it was the komatiites that followed the arc magmatism, (ii) the fact that subduction initiation around Phanerozoic plumes is not observed elsewhere argues against the plume induced subduction initiation model and (iii) more broadly, it could be argued that the location of the

FIGURE 9 | An MTZ – damp komatiite alternative model for the Caribbean Large Igneous Province. **(A,B)** Two panels for the plume-initiated subduction CLIP model of Whattam and Stern (2015), which invokes a deep mantle plume (likely the Galapagos Hot Spot) as the focus point of subduction initiation. The blue area in **(A)** is the site of slab sinking and subduction initiation around the early CLIP, following the model of Ueda et al. (2008). Brown areas in all panels are regions of active oceanic arc construction. **(C)** An endmember alternative model for an MTZ origin for the entire CLIP, based on evidence against a role for the Galapagos Hot Spot and the "coincidental" site of the CLIP in proximity to east- and west-dipping subduction zones at the gap between North and South America. **(C)** Shows the inferred location of the subducting Farallon slab just before polarity reversal and the location of the trench of the west-dipping subduction at 110 and 100 Ma (Pindell et al., 2006). The ~120 Ma Farallon initially represents an east-dipping hanging slab in the mantle as west-dipping slab of the Greater Antilles Arc (GAA) retreats, prompting the initiation of an MTZ damp plume. By 89–85 Ma, the regional slab configurations match those proposed by Whattam and Stern (2015) and define a "bowl" of inward-facing subduction that maintains a "big wedge" CLIP plume.

CLIP relative to North, Central and South America cannot be coincidental. Subduction to the north and south are key features of its geodynamic context, as is the occurrence of the Greater Antilles Arc (GAA), which is considered to have initiated at ~135 Ma (Pindell et al., 2012; Whattam and Stern, 2015). With the west dipping GAA slab and the preponderance of east dipping slabs on the North and South American margins, the location of the CLIP would be a prime candidate for big wedge processes linked to the focusing of slab material in a small volume of the MTZ (**Figure 9**). This is especially true if the suggestion of Pindell et al. (2006, 2012) involving local eastward to westward polarity reversal of subduction along the Farallon Plate is accurate. At 85 Ma in the Whattam and Stern (2015) model, the CLIP is surrounded on all sides by inward-facing subduction zones. The proposed MTZ origin of the CLIP plume readily accommodates the observations previously attributed to back arc upwelling or late upwelling of CLIP mantle in response to crustal thinning (Whattam and Stern, 2015; Dürkefälden et al., 2019). Moreover, in the MTZ model, the reason that the Galapagoes Hot Spot location through time does not match the CLIP is because it was not actually involved

in the formation of many of the terranes commonly attributed to a single LIP.

The present paper cannot provide a definitive resolution to the multiple CLIP debates. A second published CLIP scenario is considered here, however, to demonstrate that a transition zone origin for the young komatiites remains possible under a wide array of recent models. Loewen et al. (2013) also invoked a "residual Galapagos plume head" to account for the extended period of CLIP volcanism. Even if future plate reconstructions allow an initial role for the Galapagos Hot Spot, it need not be the source of the ~64 Ma Gorgona komatiites. Part of the Loewen et al. (2013) model is shown in **Figure 10** where the head of the deep mantle plume, already extended by slab roll back to the east, is decapitated by the renewed eastward subduction of the Farallon plate. Given the context of a "bowl" of active and relict subduction zones illustrated previously in **Figure 9B**, however, the geodynamic context of the CLIP at 70 Ma bears obvious similarities to the Pilbara arc-plume circuit model. Accordingly, the proposed decapitated Galapagos plume head of Loewen et al. (2013) could actually be a second plume generated in the MTZ in response to focused slab subduction.

FIGURE 10 | MTZ partial alternative to a Galapagos Hot Spot model for CLIP as applied to damp 64 Ma komatiites. **(A)** Panel from the model of Loewen et al. (2013) at 70–60 Ma. In their model, the need to have plume mantle between the subduction zones is explained by the isolation of existing CMB-derived plume head (pink) between the two subducting oceanic slabs (blue with blue arrows). If, however, evidence for a link between most of the CLIP and a core-mantle boundary plume is established beyond dispute, then this finding would not negate the potential for a big wedge plume (light blue) to generate the Gorgona komatiites, as shown in **(B)**.

CONCLUSION

A major challenge in the understanding of Archean cratons has been reconciling the apparent frequent association of plume- and arc-type sequences in the geological record. One approach has been to assert that the arc-type rocks are merely contaminated plume magmas (e.g., Barnes et al., 2012). Others have suggested that subduction may have developed around the margins of plumes or oceanic plateaus (Nair and Chacko, 2008; Ueda et al., 2008). Part of the problem may relate to the delayed acceptance of the idea that komatiite magmas contained > 0.5 wt% H_2O. Although it is logical to consider whether the water was acquired during dry plume passage through the MTZ, the earlier suggestion of Shimizu et al. (2001) of an MTZ origin for Archean plumes is at least as plausible from a petrologic perspective. It also avoids the challenge of thoroughly hydrating the dry plume and the need to reconcile MTZ water filter predictions with a damp plume reality (Bercovici and Karato, 2003; Sobolev et al., 2016). In addition, an MTZ origin for Archean plumes would be highly favored if the Archean basalt barrier concept of Davies (2008) and others is valid. The scenario would foster what Whattam and Stern (2015) referred to in the CLIP as a "plume and arc-related hybrid igneous environment," which broadly resembles the one outlined for the Abitibi belt (Ayer et al., 2002; Wyman et al., 2002).

What Wyman (2018) and the present paper have attempted to do is to accommodate the fact of damp komatiites within the geologic record of specific cratons. This approach implicates a komatiite origin from MTZ-derived plumes as the only scenario that preserves the real association of arc and plume rocks throughout the Archean. Although it is now recognized that interactions between plumes and subduction zones occurred in the Phanerozoic (Fletcher and Wyman, 2015), the association of the volcanic rock suites in cratons is far too common to be

directly analogous. Once the key concept of plume size is revised, many apparent challenges of the plume-arc interaction concept disappear, including the sporadic re-emergence of komatiitic volcanism within dominantly arc-type volcanic sequences (Ayer et al., 2002). In combination with the presence of a significant thermal boundary associated with a basalt barrier, the recent "big wedge" models provide the missing part of the puzzle as to how Archean subduction may have directly driven the temporally and spatially associated plumes. The simplicity of the MTZ plume forming mechanism ensured that komatiites could be generated throughout the Archean even as Earth moved toward a new global regime involving modern-style subduction, globe-encompassing oceanic ridge systems and tectonic plates.

In theory, the thermal boundary of the basalt barrier in the Archean might have been capable of producing small MTZ plumes anywhere on Earth. The examples considered here, however, demonstrate a close association of subduction with the well-known preserved komatiite occurrences that extends through time to Gorgona Island. This relationship is best explained if big wedge processes facilitated the formation of MTZ plumes of sufficient size to enable their ascent through the upper mantle. The evolution of early Archean cratons through a period of arc-plume circuits, driven by subduction of stagnant lid and replacement oceanic crust, has wide implications for radiogenic and stable isotope reservoirs on the early Earth. Many relatively well-preserved fractionated reservoirs could have been quite local features linked to semi-closed and long-lived (10's to 100's of m.y.) geodynamic systems. Conversely, ubiquitous weakly or unfractionated "plateau" basalts (Hollings et al., 1999) could correspond to ambient mantle leakage from outside the circuits, given that the circuits were geochemically and isotopically minor features at the global scale. The cratonic circuits may also have led to the local development of distinct habitats within isolated archipelagos where mildly oxygenated environments (etc.) developed but bore little resemblance to those found on the far more extensive stagnant lid crust. The model would also have implications for the development of Archean cratonic roots. If they were related to komatiite-generating plumes in a big wedge setting, then the roots likely formed from a mixture of residues from melting in and above the MTZ and added slab components that were commonly subject to modification during multiple arc-plume events.

The model applied to the Archean can also readily accommodate Paleoproterozoic komatiites where conflicting geodynamic interpretations also arise. It is suggested that the plumes responsible for these komatiites developed where subduction was localized around the margins of Archean cratons, and they did so prior to the demise of a basalt barrier near the base of the MTZ. Such a model is likely to have implications for early Proterozoic mobile belts and their distinctive metallogenic potential. Once the basalt barrier was gone, the frequency of komatiitic volcanism dropped markedly. The Gorgona occurrence may have required the conjunction of long-lived subduction along the west coast of the Americas and the presence of opposing contemporary subduction in the Greater Antilles Arc. The location of the Gorgona komatiites was

therefore not random but instead was the direct consequence of inward-facing subduction zones and big wedge processes.

AUTHOR CONTRIBUTIONS

The author confirms being the sole contributor of this work and has approved it for publication.

ACKNOWLEDGMENTS

REFERENCES

Andjić, G., Baumgartner, P. O., and Baumgartner-Mora, C. (2019). Collision of the caribbean large igneous province with the americas: earliest evidence from the forearc of costa rica. *Geol. Soc. Am. Bull.* 131, 1555–1580. doi: 10.1130/b35037.1

Ansdell, K. M. (2005). Tectonic evolution of the Manitoba–Saskatchewan segment of the Paleoproterozoic Trans-Hudson Orogen, Canada1,2. *Can. J. Earth Sci.* 42, 741–759. doi: 10.1139/e05-035

Arndt, N., Lesher, C. M., and Barnes, S. J. (2008). *Komatiite.* New York, NY: Cambridge University Press, 467.

Asafov, E. V., Sobolev, A. V., Gurenko, A. A., Arndt, N. T., Batanova, V. G., Portnyagin, M. V., et al. (2018). Belingwe komatiites (2.7Ga) originate from a plume with moderate water content, as inferred from inclusions in olivine. *Chem. Geol.* 478, 39–59. doi: 10.1016/j.chemgeo.2017.11.002

Ayer, J., Amelin, Y., Corfu, F., Kamo, S., Ketchum, J., Kwok, K., et al. (2002). Evolution of the southern Abitibi greenstone belt based on U–Pb geochronology: autochthonous volcanic construction followed by plutonism, regional deformation and sedimentation. *Precambrian Res.* 115, 63–95. doi: 10.1016/s0301-9268(02)00006-2

Barnes, S., Mole, D., Wyche, S., and Dering, G. (2016). Komatiites and associated rocks of the Kalgoorlie–Leonora region: geological Survey of Western Australia. *Record* 201:70.

Barnes, S. J., and Van Kranendonk, M. J. (2014). Archean andesites in the east Yilgarn craton, Australia: Products of plume-crust interaction? *Lithosphere* 6, 80–92. doi: 10.1130/l356.1

Barnes, S. J., Van Kranendonk, M. J., and Sonntag, I. (2012). Geochemistry and tectonic setting of basalts from the Eastern Goldfields Superterrane. *Aust. J. Earth Sci.* 59, 707–735. doi: 10.1080/08120099.2012.687398

Begg, G. C., Griffin, W. L., O'Reilly, S. Y., and Napatov, L. M. (2010). "Archean cratonic architecture: implications for the Yilgarn and Superior Provinces," in *Proceedings of the Fifth International Archean Symposium Abstracts*, Perth, 1–3. doi: 10.5382/rev.11.12

Bercovici, D., and Karato, S.-I. (2003). Whole-mantle convection and the transition-zone water filter. *Nature* 425, 39–44. doi: 10.1038/nature01918

Bleeker, W., and Kamo, S. L. (2018). "Extent, origin, and deposit-scale controls of the 1883 Ma Circum-Superior large igneous province, northern Manitoba, Ontar-io, Quebec, Nunavut and Labrador," in *Targeted Geoscience Initiative: 2017 report of activities*, ed. N. Rogers (Orléans: Geological Survey of Canada), 5–14.

Boschman, L. M., van Hinsbergen, D. J. J., Torsvik, T. H., Spakman, W., and Pindell, J. L. (2014). Kinematic reconstruction of the caribbean region since the early jurassic. *Earth Sci. Rev.* 138, 102–136. doi: 10.1016/j.earscirev.2014.08.007

Bouquain, S., Arndt, N. T., Faure, F., and Libourel, G. (2014). An experimental study of pyroxene crystallization during rapid cooling in a thermal gradient: application to komatiites. *Solid Earth* 5, 641–650. doi: 10.5194/se-5-641-2014

Bredow, E., Steinberger, B., Gassmöller, R., and Dannberg, J. (2017). How plume-ridge interaction shapes the crustal thickness pattern of the Réunion hotspot track. *Geochem. Geophys. Geosyst.* 18, 2930–2948. doi: 10.1002/2017gc006875

Campbell, I. H., and Griffiths, R. W. (1990). Implications of mantle plume structure for the evolution of flood basalts. *Earth Planet. Sci. Lett.* 99, 79–93. doi: 10.1016/0012-821x(90)90072-6

Campbell, I. H., and Griffiths, R. W. (1992). The changing nature of mantle hotspots through time: implications for the chemical evolution of the mantle. *J. Geol.* 100, 497–523. doi: 10.1086/629605

Campbell, I. H., and Griffiths, R. W. (1993). The evolution of the mantle's chemical structure. *Lithos* 30, 389–399.

Campbell, I. H., and Griffiths, R. W. (2014). Did the formation of D" cause the Archaean–Proterozoic transition? *Earth Planet. Sci. Lett.* 388, 1–8. doi: 10.1016/j.epsl.2013.11.048

Campbell, I. H., Griffiths, R. W., and Hill, R. I. (1989). Melting in an Archaean mantle plume: heads it's basalts, tails it's komatiites. *Nature* 339, 697–699. doi: 10.1038/339697a0

Campbell, I. H., and Hill, R. I. (1988). A two-stage model for the formation of the granite-greenstone terrains of the Kalgoorlie-Norseman area, Western Australia. *Earth Planet. Sci. Lett.* 90, 11–25. doi: 10.1016/0012-821x(88)90107-0

Cassidy, K. F., Barley, M. E., Groves, D. I., Perring, C. S., and Hallberg, J. A. (1991). An overview of the nature, distribution and inferred tectonic setting of granitoids in the late-Archaean Norseman-Wiluna Belt. *Precambrian Res.* 51, 51–83. doi: 10.1016/0301-9268(91)90094-q

Cassidy, K. F., and Wyche, S. (2012). Thematic Issue: Archean Evolution—Yilgarn Craton. *Aust. J. Earth Sci.* 59, 599–601. doi: 10.1080/08120099.2012.704882

Choi, E., Fiorentini, M. L., Giuliani, A., Foley, S. F., Maas, R., and Taylor, W. R. (2020). Subduction-related petrogenesis of Late Archean calc-alkaline lamprophyres in the Yilgarn Craton (Western Australia). *Precambrian Res.* 338:105550. doi: 10.1016/j.precamres.2019.105550

Ciborowski, T. J. R., Minifie, M. J., Kerr, A. C., Ernst, R. E., Baragar, B., and Millar, I. L. (2017). A mantle plume origin for the Palaeoproterozoic Circum-Superior Large Igneous Province. *Precambrian Res.* 294, 189–213. doi: 10.1016/j.precamres.2017.03.001

Claoué-Long, J. C., Compston, W., and Cowden, A. (1988). The age of the Kambalda greenstones resolved by ion-microprobe: implications for Archaean dating methods. *Earth Planet. Sci. Lett.* 89, 239–259. doi: 10.1016/0012-821x(88)90175-6

Corfu, F. (1993). The evolution of the Southern Abitibi greenstone belt in light of precise U-Pb geochronology. *Econ. Geol.* 88, 1323–1340. doi: 10.2113/gsecongeo.88.6.1323

Corrigan, D., Pehrsson, S., Wodicka, N., and de Kemp, E. (2009). The Palaeoproterozoic Trans-Hudson Orogen: a prototype of modern accretionary processes. *Geol. Soc. Lond. Spec. Publ.* 327, 457–479. doi: 10.1144/sp327.19

Courtillot, V., Davaille, A., Besse, J., and Stock, J. (2003). Three distinct types of hotspots in the Earth's mantle. *Earth Planet. Sci. Lett.* 205, 295–308. doi: 10.1016/s0012-821x(02)01048-8

Czarnota, K., Champion, D. C., Goscombe, B., Blewett, R. S., Cassidy, K. F., Henson, P. A., et al. (2010). Geodynamics of the eastern Yilgarn Craton. *Precambrian Res.* 183, 175–202. doi: 10.1016/j.precamres.2010.08.004

Czas, J., Pearson, D. G., Stachel, T., Kjarsgaard, B. A., and Read, G. H. (2020). A Palaeoproterozoic diamond-bearing lithospheric mantle root beneath the Archean Sask Craton, Canada. *Lithos* 356-357:105301. doi: 10.1016/j.lithos.2019.105301

Davies, G. F. (1995). Punctuated tectonic evolution of the earth. *Earth Planet. Sci. Lett.* 136, 363–379. doi: 10.1016/0012-821x(95)00167-b

Davies, G. F. (2008). Episodic layering of the early mantle by the 'basalt barrier' mechanism. *Earth Planet. Sci. Lett.* 275, 382–392. doi: 10.1016/j.epsl.2008.08.036

Dostal, J., and Mueller, W. U. (1997). Komatiite Flooding of a Rifted Archean Rhyolitic Arc Complex: geochemical Signature and Tectonic Significance of the Stoughton-Roquemaure Group, Abitibi Greenstone Belt, Canada. *J. Geol.* 105, 545–564. doi: 10.1086/515956

Dostal, J., and Mueller, W. U. (2013). Deciphering an Archean mantle plume: Abitibi greenstone belt, Canada. *Gondwana Res.* 23, 493–505. doi: 10.1016/j.gr.2012.02.005

Dürkefälden, A., Hoernle, K., Hauff, F., Werner, R., and Garbe-Schönberg, D. (2019). Second-stage Caribbean Large Igneous Province volcanism: the depleted icing on the enriched cake. *Chem. Geol.* 509, 45–63. doi: 10.1016/j.chemgeo.2019.01.004

Egan, J. F. B. (2020). *The Deflector Au–Cu Deposit: Defining an Anomalous Yilgarn Craton Mineralisation Style Using Trace Element Geochemistry*. East Perth: Geological Survey of Western Australia.

Evans, D. A. D., and Halls, H. C. (2010). Restoring Proterozoic deformation within the Superior craton. *Precambrian Res.* 183, 474–489. doi: 10.1016/j.precamres.2010.02.007

Faccenna, C., Becker, T. W., Lallemand, S., Lagabrielle, Y., Funiciello, F., and Piromallo, C. (2010). Subduction-triggered magmatic pulses: a new class of plumes? *Earth Planet. Sci. Lett.* 299, 54–68. doi: 10.1016/j.epsl.2010.08.012

Farnetani, C. G., Legras, B., and Tackley, P. J. (2002). Mixing and deformations in mantle plumes. *Earth Planet. Sci. Lett.* 196, 1–15. doi: 10.1016/s0012-821x(01)00597-0

Farnetani, C. G., and Samuel, H. (2005). Beyond the thermal plume paradigm. *Geophys. Res. Lett.* 32:L07311.

Fitton, J. G., Saunders, A. D., Norry, M. J., Hardarson, B. S., and Taylor, R. N. (1997). Thermal and chemical structure of the Iceland plume. *Earth Planet. Sci. Lett.* 153, 197–208. doi: 10.1016/s0012-821x(97)00170-2

Fletcher, M., and Wyman, D. A. (2015). Mantle plume–subduction zone interactions over the past 60 Ma. *Lithos* 233, 162–173. doi: 10.1016/j.lithos.2015.06.026

Fletcher, M., Wyman, D. A., and Zahirovic, S. (2020). Mantle plumes, triple junctions and transforms: a reinterpretation of Pacific Cretaceous – Tertiary LIPs and the Laramide connection. *Geosci. Front.* 11, 1133–1144. doi: 10.1016/j.gsf.2019.09.003

Geng, X., Foley, S. F., Liu, Y., Wang, Z., Hu, Z., and Zhou, L. (2019). Thermal-chemical conditions of the North China Mesozoic lithospheric mantle and implication for the lithospheric thinning of cratons. *Earth Planet. Sci. Lett.* 516, 1–11. doi: 10.1016/j.epsl.2019.03.012

Goes, S., Agrusta, R., van Hunen, J., and Garel, F. (2017). Subduction-transition zone interaction: a review. *Geosphere* 13:644. doi: 10.1130/ges01476.1

Green, D. H., Nicholls, I. A., Viljoen, M., and Viljoen, R. (1975). Experimental demonstration of the existence of peridotitic liquids in earliest archean magmatism. *Geology* 3, 11–14. doi: 10.1130/0091-7613(1975)3<11:edoteo>2.0.co;2

Griffin, W. L., Belousova, E. A., O'Neill, C., O'Reilly, S. Y., Malkovets, V., Pearson, N. J., et al. (2014). The world turns over: Hadean–Archean crust–mantle evolution. *Lithos* 189, 2–15. doi: 10.1016/j.lithos.2013.08.018

Griffin, W. L., O'Reilly, S. Y., Abe, N., Aulbach, S., Davies, R. M., Pearson, N. J., et al. (2003). The origin and evolution of Archean lithospheric mantle. *Precambrian Res.* 127, 19–41. doi: 10.1016/s0301-9268(03)00180-3

Grove, T. L., and Parman, S. W. (2004). Thermal evolution of the Earth as recorded by komatiites. *Earth Planet. Sci. Lett.* 219, 173–187. doi: 10.1016/s0012-821x(04)00002-0

Gruau, G., Chauvel, C., Arndt, N. T., and Cornichet, J. (1990). Aluminum depletion in komatiites and garnet fractionation in the early Archean mantle: hafnium isotopic constraints. *Geochim. Cosmochim. Acta* 54, 3095–3101. doi: 10.1016/0016-7037(90)90125-5

Gurenko, A. A., and Kamenetsky, V. S. (2011). Boron isotopic composition of olivine-hosted melt inclusions from Gorgona komatiites, Colombia: New evidence supporting wet komatiite origin. *Earth Planet. Sci. Lett.* 312, 201–212. doi: 10.1016/j.epsl.2011.09.033

Hansen, V. L. (2007). Subduction origin on early Earth: a hypothesis. *Geology* 35:1059. doi: 10.1130/g24202a.1

Hauff, F., Hoernle, K., Tilton, G., Graham, D. W., and Kerr, A. C. (2000). Large volume recycling of oceanic lithosphere over short time scales: geochemical constraints from the Caribbean Large Igneous Province. *Earth Planet. Sci. Lett.* 174, 247–263. doi: 10.1016/s0012-821x(99)00272-1

Hayman, P. C., Thébaud, N., Pawley, M. J., Barnes, S. J., Cas, R. A. F., Amelin, Y., et al. (2015). Evolution of a 2.7 Ga large igneous province: A volcanological, geochemical and geochronological study of the Agnew Greenstone Belt, and new regional correlations for the Kalgoorlie Terrane (Yilgarn Craton, Western Australia). *Precambrian Res.* 270, 334–368. doi: 10.1016/j.precamres.2015.09.016

He, X.-F., Santosh, M., and Ganguly, S. (2017). Mesozoic felsic volcanic rocks from the North China craton: intraplate magmatism associated with craton destruction. *Geol. Soc. Am. Bull.* 129, 947–969. doi: 10.1130/B31607.1

Heaman, L. M., Peck, D., and Toope, K. (2009). Timing and geochemistry of 1.88Ga Molson Igneous Events, Manitoba: insights into the formation of a craton-scale magmatic and metallogenic province. *Precambrian Res.* 172, 143–162. doi: 10.1016/j.precamres.2009.03.015

Herzberg, C. (1999). "Phase equilibrium constraints on the formation of cratonic mantle," in *Mantle Petrology: Field Observations and High Pressure Experimentation: A Tribute to Francis R. (Joe)*, eds Y. Fei, C. Bertka, and B. O. Mysen (Boyd: Geochemical Society Special Publication), 241–257.

Herzberg, C. (2016). Petrological evidence from komatiites for an early earth carbon and water cycle. *J. Petrol.* 57, 2271–2288. doi: 10.1093/petrology/egw055

Herzberg, C. T. (1993). Lithosphere peridotites of the Kaapvaal craton. *Earth Planet. Sci. Lett.* 120, 13–29. doi: 10.1016/0012-821x(93)90020-a

Hickman, A., and Van Kranendonk, M. (2012). A billion years of Earth history: a geological transect through the Pilbara Craton and the Mount Bruce Supergroup — a field guide to accompany 34th IGC Excursion WA-2: geological Survey of Western Australia. *Record* 201:66.

Hill, R. I., Chappell, B. W., and Campbell, I. H. (1992). Late Archaean granites of the southeastern Yilgarn Block, Western Australia: age, geochemistry, and origin. *Earth Environ. Sci. Trans. R Soc. Edinb.* 83, 211–226. doi: 10.1017/S0263593300007902

Hollings, P., Wyman, D., and Kerrich, R. (1999). Komatiite-basalt-rhyolite volcanic associations in Northern Superior Province greenstone belts: Significance of plume-arc interaction in the generation of the proto continental Superior Province. *Lithos* 46, 137–161. doi: 10.1016/s0024-4937(98)00058-9

Holt, A. F., Royden, L. H., and Becker, T. W. (2017). The dynamics of double slab subduction. *Geophys. J. Int.* 209, 250–265.

Humbert, F., Elburg, M. A., Ossa, F. O., de Kock, M. O., and Robion, P. (2018). Variolites of the Paleoproterozoic Hekpoort Formation (Transvaal sub-basin, Kaapvaal craton): Multistage undercooling textures? *Lithos* 316-317, 48–65. doi: 10.1016/j.lithos.2018.07.005

Kamber, B. S. (2015). The evolving nature of terrestrial crust from the Hadean, through the Archean, into the Proterozoic. *Precambrian Res.* 258, 48–82. doi: 10.1016/j.precamres.2014.12.007

Kamber, B. S., and Tomlinson, E. L. (2019). Petrological, mineralogical and geochemical peculiarities of Archaean cratons. *Chem. Geol.* 511, 123–151. doi: 10.1016/j.chemgeo.2019.02.011

Kamenetsky, V. S., Gurenko, A. A., and Kerr, A. C. (2010). Composition and temperature of komatiite melts from Gorgona Island, Colombia, constrained from olivine-hosted melt inclusions. *Geology* 38, 1003–1006. doi: 10.1130/g31143.1

Kastek, N., Ernst, R. E., Cousens, B. L., Kamo, S. L., Bleeker, W., Söderlund, U., et al. (2018). U-Pb Geochronology and Geochemistry of the Povungnituk Group of the Cape Smith Belt: Part of a Craton-Scale Circa 2.0Ga Minto-Povungnituk Large Igneous Province, Northern Superior Craton. *Lithos* 320-321, 315–331. doi: 10.1016/j.lithos.2018.09.026

Kerr, A. C., and Tarney, J. (2005). Tectonic evolution of the Caribbean and northwestern South America: the case for accretion of two Late Cretaceous oceanic plateaus. *Geology* 33, 269–272. doi: 10.1130/g21109.1

Kerrich, R., and Wyman, D. (1990). Geodynamic setting of mesothermal gold deposits: an association with accretionary tectonic regimes. *Geology* 18, 882–885. doi: 10.1130/0091-7613(1990)018<0882:gsomgd>2.3.co;2

Ketchum, J. W. F., Culshaw, N. G., and Barr, S. M. (2002). Anatomy and orogenic history of a Paleoproterozoic accretionary belt: the Makkovik Province, Labrador, Canada1. *Can. J. Earth Sci.* 39, 711–730. doi: 10.1139/e01-099

Kositcin, N., Brown, S. J. A., Barley, M. E., Krapez, B., Cassidy, K. F., and Champion, D. C. (2008). SHRIMP U-Pb zircon age constraints on the Late Archaean tectonostratigraphic architecture of the Eastern Goldfields Superterrane, Yilgarn Craton, Western Australia. *Precambrian Res.* 161, 5–33. doi: 10.1016/j.precamres.2007.06.018

Li, S.-G., Yang, W., Ke, S., Meng, X., Tian, H., Xu, L., et al. (2017). Deep carbon cycles constrained by a large-scale mantle Mg isotope anomaly in eastern China. *Natl. Sci. Rev.* 4, 111–120. doi: 10.1093/nsr/nww070

Loewen, M. W., Duncan, R. A., Kent, A. J. R., and Krawl, K. (2013). Prolonged plume volcanism in the Caribbean Large Igneous Province: new insights from Curaçao and Haiti. *Geochem. Geophys. Geosyst.* 14, 4241–4259. doi: 10.1002/ggge.20273

Long, X., Ballmer, M. D., Córdoba, A. M. C., and Li, C.-F. (2019). Mantle Melting and Intraplate Volcanism Due to Self-Buoyant Hydrous Upwellings From the Stagnant Slab That Are Conveyed by Small-Scale Convection. *Geochem. Geophys. Geosyst.* 20, 4972–4997. doi: 10.1029/2019gc008591

Lowrey, J. R., Ivanic, T. J., Wyman, D. A., and Roberts, M. P. (2017). Platy pyroxene: new insights into spinifex texture. *J. Petrol.* 58, 1671–1700. doi: 10.1093/petrology/egx069

Lowrey, J. R., Wyman, D. A., Ivanic, T. J., Smithies, R. H., and Maas, R. (2020). Archean boninite-like rocks of the Northwestern Youanmi Terrane, Yilgarn Craton: Geochemistry and Genesis. *J. Petrol.* 60, 2131–2168. doi: 10.1093/petrology/egaa002

Martin, D. M., Hocking, R. M., Riganti, R. M. A., and Tyler, I. M. (2015). *Geological Map of Western Australia, 1:2 500 000*, 14th Edn. Perth, WA: Geological Survey of Western Australia.

Maruyama, S., Hasegawa, A., Santosh, M., Kogiso, T., Omori, S., Nakamura, H., et al. (2009). The dynamics of big mantle wedge, magma factory, and metamorphic–metasomatic factory in subduction zones. *Gondwana Res.* 16, 414–430. doi: 10.1016/j.gr.2009.07.002

McDonough, W. F., and Sun, S. S. (1995). The composition of the Earth. *Chem. Geol.* 120, 223–253.

Mittelstaedt, E., and Ito, G. (2005). Plume-ridge interaction, lithospheric stresses, and the origin of near-ridge volcanic lineaments. *Geochem. Geophys. Geosyst.* 6, 1–20.

Mjelde, R., Wessel, P., and Müller, R. D. (2010). Global pulsations of intraplate magmatism through the Cenozoic. *Lithosphere* 2, 361–376. doi: 10.1130/l107.1

Mole, D. R., Fiorentini, M. L., Cassidy, K. F., Kirkland, C. L., Thebaud, N., McCuaig, T. C., et al. (2015). Crustal evolution, intra-cratonic architecture and the metallogeny of an Archaean craton. *Geol. Soc. Lond. Spec. Publ.* 393, 23–80. doi: 10.1144/sp393.8

Mole, D. R., Fiorentini, M. L., Thebaud, N., Cassidy, K. F., McCuaig, T. C., Kirkland, C. L., et al. (2014). Archean komatiite volcanism controlled by the evolution of early continents. *Proc. Natl. Acad. Sci. U.S.A.* 111, 10083–10088. doi: 10.1073/pnas.1400273111

Mueller, W. U., Stix, J., Corcoran, P. L., and Daigneault, R. (2009). Subaqueous calderas in the Archean Abitibi greenstone belt: an overview and new ideas. *Ore Geol. Rev.* 35, 4–46. doi: 10.1016/j.oregeorev.2008.12.003

Nair, R., and Chacko, T. (2008). Role of oceanic plateaus in the initiation of subduction and origin of continental crust. *Geology* 36, 583–586. doi: 10.1130/g24773a.1

Namiki, A., Sueyoshi, K., and Takeuchi, N. (2013). Can a sheet-like low-velocity region form an elongated Large Igneous Province? *Geochem. Geophys. Geosyst.* 14, 3053–3066. doi: 10.1002/ggge.20182

Nelson, D. R. (2001). *Compilation of Geochronological Data, 2000*. (Perth, WA: Geological Survey of Western Australia), 78–89.

Nelson, P. L., and Grand, S. P. (2018). Lower-mantle plume beneath the Yellowstone hotspot revealed by core waves. *Nat. Geosci.* 11, 280–284. doi: 10.1038/s41561-018-0075-y

Osozawa, S., Shinjo, R., Lo, C.-H., Jahn, B.-M., Hoang, N., Sasaki, M., et al. (2012). Geochemistry and geochronology of the Troodos ophiolite: An SSZ ophiolite generated by subduction initiation and an extended episode of ridge subduction? *Lithosphere* 4, 497–510. doi: 10.1130/l205.1

Pawley, M. J., Wingate, M. T. D., Kirkland, C. L., Wyche, S., Hall, C. E., Romano, S. S., et al. (2012). Adding pieces to the puzzle: episodic crustal growth and a new terrane in the northeast Yilgarn Craton, Western Australia. *Aust. J. Earth Sci.* 59, 603–623. doi: 10.1080/08120099.2012.696555

Pearce, J. A., and Reagan, M. K. (2019). Identification, classification, and interpretation of boninites from Anthropocene to Eoarchean using Si-Mg-Ti systematics. *Geosphere* 15, 1008–1037. doi: 10.1130/ges01661.1

Percival, J. A., Skulski, T., Sanborn-Barrie, M., Stott, G. M., Leclair, A. D., Corkery, M. T., et al. (2012). "Geology and Tectonic Evolution of the Superior Province, Canada," in *Tectonic Styles in Canada: The LITHOPROBE Perspective*, eds J. A. Percival, F. A. Cook, and R. M. Clowes (St. John's: Geological Association of Canada), 321–378.

Percival, J. A., Whalen, J. B., and Rayner, N. (2005). *Pikwitonei–Snow Lake Manitoba Transect (parts of NTS 63J, 63O and 63P), Trans-Hudson Orogen– Superior Margin Metallotect Project: New Results and Tectonic Interpretation, Report of Activities 2005. Manitoba Geological Survey*. Available online at: https://www.gov.mb.ca/iem/geo/field/roa04pdfs/GS-11.pdf (accessed June 18, 2020).

Perry, H. K. C., Mareschal, J. C., and Jaupart, C. (2006). Variations of strength and localized deformation in cratons: the 1.9 Ga Kapuskasing uplift, Superior Province, Canada. *Earth Planet. Sci. Lett.* 249, 216–228. doi: 10.1016/j.epsl.2006.07.013

Pindell, J., Kennan, L., Stanek, K. P., Maresh, W. V., and Draper, G. (2006). Foundations of Gulf of Mexico and Caribbean evolution: eight controversies resolved. *Geol. Acta* 4, 303–341.

Pindell, J., Maresch, W. V., Martens, U., and Stanek, K. (2012). The Greater Antillean Arc: early Cretaceous origin and proposed relationship to Central American subduction mélanges: implications for models of Caribbean evolution. *Int. Geol. Rev.* 54, 131–143. doi: 10.1080/00206814.2010.510008

Rey, P. F., Coltice, N., and Flament, N. (2014). Spreading continents kick-started plate tectonics. *Nature* 513, 405–408. doi: 10.1038/nature13728

Rolf, T., and Tackley, P. J. (2011). Focussing of stress by continents in 3D spherical mantle convection with self-consistent plate tectonics. *Geophys. Res. Lett.* 38:L18301.

Schulz, K. J., and Cannon, W. F. (2007). The Penokean orogeny in the Lake Superior region. *Precambrian Res.* 157, 4–25. doi: 10.1016/j.precamres.2007.02.022

Serrano, L., Ferrari, L., Martínez, M. L., Petrone, C. M., and Jaramillo, C. (2011). An integrative geologic, geochronologic and geochemical study of Gorgona Island, Colombia: implications for the formation of the Caribbean Large Igneous Province. *Earth Planet. Sci. Lett.* 309, 324–336. doi: 10.1016/j.epsl.2011.07.011

Seton, M., Müller, R. D., Zahirovic, S., Gaina, C., Torsvik, T., Shephard, G., et al. (2012). Global continental and ocean basin reconstructions since 200 Ma. *Earth Sci. Rev.* 113, 212–270. doi: 10.1016/j.earscirev.2012.03.002

Shimizu, K., Komiya, T., Hirose, K., Shimizu, N., and Maruyama, S. (2001). Cr-spinel, an excellent micro-container for retaining primitive melts – implications for a hydrous plume origin for komatiites. *Earth Planet. Sci. Lett.* 189, 177–188. doi: 10.1016/s0012-821x(01)00359-4

Smithies, R. H. (2000). The Archaean tonalite-trondhjemite-granodiorite (TTG) series is not an analogue of Cenozoic adakite. *Earth Planet. Sci. Lett.* 182, 115–125. doi: 10.1016/s0012-821x(00)00236-3

Smithies, R. H. (2002). Archaean boninite-like rocks in an intracratonic setting. *Earth Planet. Sci. Lett.* 197, 19–34. doi: 10.1016/s0012-821x(02)00464-8

Smithies, R. H., and Champion, D. C. (2000). The Archaean high-Mg diorite suite: links to Tonalite-Trondhjemite-Granodiorite magmatism and implications for early Archaean crustal growth. *J. Petrol.* 41, 1653–1671. doi: 10.1093/petrology/41.12.1653

Smithies, R. H., Champion, D. C., and Van Kranendonk, M. J. (2009). Formation of Paleoarchean continental crust through infracrustal melting of enriched basalt. *Earth Planet. Sci. Lett.* 281, 298–306. doi: 10.1016/j.epsl.2009.03.003

Smithies, R. H., Ivanic, T. J., Lowrey, J. R., Morris, P. A., Barnes, S. J., Wyche, S., et al. (2018). Two distinct origins for Archean greenstone belts. *Earth Planet. Sci. Lett.* 487, 106–116.

Smithies, R. H., Van Kranendonk, M. J., and Champion, D. C. (2005). It started with a plume - Early Archaean basaltic proto-continental crust. *Earth Planet. Sci. Lett.* 238, 284–297. doi: 10.1016/j.epsl.2005.07.023

Sobolev, A. V., Asafov, E. V., Gurenko, A. A., Arndt, N. T., Batanova, V. G., Portnyagin, M. V., et al. (2016). Komatiites reveal a hydrous Archaean deep-mantle reservoir. *Nature* 531, 628–632. doi: 10.1038/nature17152

Sobolev, A. V., Asafov, E. V., Gurenko, A. A., Arndt, N. T., Batanova, V. G., Portnyagin, M. V., et al. (2019). Deep hydrous mantle reservoir provides evidence for crustal recycling before 3.3 billion years ago. *Nature* 571, 555–559. doi: 10.1038/s41586-019-1399-5

Spaggiari, C. V., Pidgeon, R. T., and Wilde, S. A. (2007). The Jack Hills greenstone belt, Western Australia: Part 2: lithological relationships and implications for the deposition of = 4.0 Ga detrital zircons. *Precambrian Res.* 155, 261–286. doi: 10.1016/j.precamres.2007.02.004

Stampfli, G. M., and Borel, G. D. (2002). A plate tectonic model for the Paleozoic and Mesozoic constrained by dynamic plate boundaries and restored synthetic oceanic isochrons. *Earth Planet. Sci. Lett.* 196, 17–33. doi: 10.1016/s0012-821x(01)00588-x

Stern, R. J., and Gerya, T. (2018). Subduction initiation in nature and models: a review. *Tectonophysics* 746, 173–198. doi: 10.1016/j.tecto.2017.10.014

St-Onge, M. R., Wodicka, N., and Ijewliw, O. (2006). Polymetamorphic Evolution of the Trans-Hudson Orogen, Baffin Island, Canada: integration of Petrological, Structural and Geochronological Data. *J. Petrol.* 48, 271–302. doi: 10.1093/petrology/egl060

Sun, S. S., and Nesbitt, R. W. (1978). Petrogenesis of Archean ultrabasic and basic volcanics: evidence from rare earth elements. *Contrib. Mineral. Petrol.* 65, 301–325. doi: 10.1007/bf00375516

Trela, J., Gazel, E., Sobolev, A. V., Moore, L., Bizimis, M., Jicha, B., et al. (2017). The hottest lavas of the Phanerozoic and the survival of deep Archaean reservoirs. *Nat. Geosci.* 10, 451–456. doi: 10.1038/ngeo2954

Ueda, K., Gerya, T., and Sobolev, S. V. (2008). Subduction initiation by thermal–chemical plumes: numerical studies. *Phys. Earth Planet. Inter.* 171, 296–312. doi: 10.1016/j.pepi.2008.06.032

van Hunen, J., and Moyen, J.-F. (2012). Archean Subduction: Fact or Fiction? *Annu. Rev. Earth Planet. Sci.* 40, 195–219. doi: 10.1146/annurev-earth-042711-105255

Van Kranendonk, M.J., Hickman, A.H., Smithes, R.H., Nelson, D.R., Pike, G. (2002). Geology and tectonic evolution of the Archean North Pilbara Terrain, Pilbara Craton, Western Australia. *Econ. Geol.* 97, 695–732. doi: 10.2113/gsecongeo.97.4.695

Van Kranendonk, M. J., Ivanic, T. J., Wingate, M. T. D., Kirkland, C. L., and Wyche, S. (2013). Long-lived, autochthonous development of the Archean Murchison Domain, and implications for Yilgarn Craton tectonics. *Precambrian Res.* 229, 49–92. doi: 10.1016/j.precamres.2012.08.009

Van Kranendonk, M. J., Smithies, R. H., Hickman, A. H., and Champion, D. C. (2007). "Chapter 4.1 Paleoarchean Development of a Continental Nucleus: the East Pilbara Terrane of the Pilbara Craton, Western Australia," in *Developments in Precambrian Geology*, eds M. J. Van Kranendonk, R. H. Smithies, and V. C. Bennett (Amsterdam: Elsevier), 307–337. doi: 10.1016/s0166-2635(07)15041-6

Van Kranendonk, M. J., Smithies, R. H., Hickman, A. H., Wingate, M. T. D., and Bodorkos, S. (2010). Evidence for Mesoarchean (˜ 3.2 Ga) rifting of the Pilbara Craton: the missing link in an early Precambrian Wilson cycle. *Precambrian Res.* 177, 145–161. doi: 10.1016/j.precamres.2009.11.007

Viljoen, M. J., and Viljoen, R. P. (1969). Evidence for the existence of a mobile extrusive peridotitic magma from the Komati Formation of the Onverwacht Group. *Geol. Soc. S. Afr. Spec. Publ.* 21, 87–112.

Wang, Q., Schiøtte, L., and Campbell, I. H. (1998). Geochronology of supracrustal rocks from the Golden Grove area, Murchison Province, Yilgarn Craton, Western Australia. *Aust. J. Earth Sci.* 45, 571–577. doi: 10.1080/08120099808728413

Wang, Q., Wyman, D. A., Xu, J. F., Zhao, Z. H., Jian, P., and Zi, F. (2007). Partial melting of thickened or delaminated lower crust in the Middle of eastern China: implications for Cu-Au mineralization. *J. Geol.* 115, 149–161. doi: 10.1086/510643

Wang, X.-C., Wilde, S. A., Li, Q.-L., and Yang, Y.-N. (2015). Continental flood basalts derived from the hydrous mantle transition zone. *Nat. Commun.* 6:7700.

Wang, Z., Kusky, T. M., and Capitanio, F. A. (2016). Lithosphere thinning induced by slab penetration into a hydrous mantle transition zone. *Geophys. Res. Lett.* 43, 11567–11577.

Waterton, P., Pearson, D. G., Kjarsgaard, B., Hulbert, L., Locock, A., Parman, S., et al. (2017). Age, origin, and thermal evolution of the ultra-fresh ˜ 1.9 Ga Winnipegosis Komatiites, Manitoba, Canada. *Lithos* 268-271, 114–130. doi: 10.1016/j.lithos.2016.10.033

Weller, O. M., and St-Onge, M. R. (2017). Record of modern-style plate tectonics in the Palaeoproterozoic Trans-Hudson orogen. *Nat. Geosci.* 10, 305–311. doi: 10.1038/ngeo2904

Whattam, S. A., and Stern, R. J. (2015). Late Cretaceous plume-induced subduction initiation along the southern margin of the Caribbean and NW South America: the first documented example with implications for the onset of plate tectonics. *Gondwana Res.* 27, 38–63. doi: 10.1016/j.gr.2014.07.011

Whitford, D. J., and Ashley, P. M. (1992). The Scuddles volcanic-hosted massive sulfide deposit, Western Australia; geochemistry of the host rocks and evaluation of lithogeochemistry for exploration. *Econ. Geol.* 87, 873–888. doi: 10.2113/gsecongeo.87.3.873

Wiemer, D., Schrank, C. E., Murphy, D. T., Wenham, L., and Allen, C. M. (2018). Earth's oldest stable crust in the Pilbara Craton formed by cyclic gravitational overturns. *Nat. Geosci.* 11, 357–361. doi: 10.1038/s41561-018-0105-9

Wilde, S. A., Middleton, M. F., and Evans, B. J. (1996). Terrane accretion in the southwestern Yilgarn Craton: evidence from a deep seismic crustal profile. *Precambrian Res.* 78, 179–196. doi: 10.1016/0301-9268(95)00077-1

Wilson, A. H., and Versfeld, J. A. (1994). The early Archaean Nondweni greenstone belt, southern Kaapvaal Craton, South Africa, Part II. Characteristics of the volcanic rocks and constraints on magma genesis. *Precambrian Res.* 67, 277–320. doi: 10.1016/0301-9268(94)90013-2

Wilson, A. H., Versfeld, J. A., and Hunter, D. R. (1989). Emplacement, crystallization and alteration of spinifex-textured komatiitic basalt flows in the Archaean Nondweni greenstone belt, southern Kaapvaal Craton, South Africa. *Contrib. Mineral. Petrol.* 101, 301–317. doi: 10.1007/bf00375315

Witt, W. K., Cassidy, K. F., Lu, Y.-J., and Hagemann, S. G. (2018). The tectonic setting and evolution of the 2.7 Ga Kalgoorlie–Kurnalpi Rift, a world-class Archean gold province. *Miner. Depos.* 55, 601–631. doi: 10.1007/s00126-017-0778-9

Wittig, N., Webb, M., Pearson, D. G., Dale, C. W., Ottley, C. J., Hutchison, M., et al. (2010). Formation of the North Atlantic Craton: timing and mechanisms constrained from Re–Os isotope and PGE data of peridotite xenoliths from S.W. Greenland. *Chem. Geol.* 276, 166–187. doi: 10.1016/j.chemgeo.2010.06.002

Wyman, D. (2018). Do cratons preserve evidence of stagnant lid tectonics? *Geosci. Front.* 9, 3–17. doi: 10.1016/j.gsf.2017.02.001

Wyman, D., and Kerrich, R. (1988). Alkaline magmatism, major structures, and gold deposits: implications for greenstone belt gold metallogeny. *Econ. Geol.* 83, 454–461. doi: 10.2113/gsecongeo.83.2.454

Wyman, D. A. (2003). Upper mantle processes beneath the 2.7 Ga Abitibi belt, Canada: a trace element perspective. *Precambrian Res.* 127, 143–165. doi: 10.1016/s0301-9268(03)00185-2

Wyman, D. A. (2013). A critical assessment of neoarchean "plume only" geodynamics: evidence from the Superior Province. *Precambrian Res.* 229, 3–19. doi: 10.1016/j.precamres.2012.01.010

Wyman, D. A. (2019). 2.8Ga Subduction-related magmatism in the Youanmi Terrane and a revised geodynamic model for the Yilgarn Craton. *Precambrian Res.* 327, 14–33. doi: 10.1016/j.precamres.2019.02.008

Wyman, D. A., and Hollings, P. (2006). "Late Archean convergent margin volcanism in the Superior Province: a comparison of the Blake River Group and Confederation Assemblage," in *Archean Geodynamics and Environments, AGU Geophysical Monograph Series*, eds K. Benn, J.-C. Mareschal, and K. Condie (Washington, DC: American Geophysical Union), 215–238. doi: 10.1029/164gm14

Wyman, D. A., Hollings, P., and Conceição, R. V. (2015). Geochemistry and radiogenic isotope characteristics of xenoliths in Archean diamondiferous lamprophyres: implications for the Superior Province cratonic keel. *Lithos* 233, 111–130. doi: 10.1016/j.lithos.2015.02.018

Wyman, D. A., and Kerrich, R. (2002). Formation of Archean continental lithospheric roots: the role of mantle plumes. *Geology* 30, 543–546. doi: 10.1130/0091-7613(2002)030<0543:foaclr>2.0.co;2

Wyman, D. A., and Kerrich, R. (2012). Geochemical and isotopic characteristics of Youanmi terrane volcanism: the role of mantle plumes and subduction tectonics in the western Yilgarn Craton. *Aust. J. Earth Sci.* 59, 671–694. doi: 10.1080/08120099.2012.702684

Wyman, D. A., Kerrich, R., and Polat, A. (2002). Assembly of Archean cratonic mantle lithosphere and crust: plume-arc interaction in the Abitibi-Wawa subduction-accretion complex. *Precambrian Res.* 115, 37–62. doi: 10.1016/s0301-9268(02)00005-0

Yang, J., Zhao, L., Kaus, B. J. P., Lu, G., Wang, K., and Zhu, R. (2018). Slab-triggered wet upwellings produce large volumes of melt: insights into the destruction of the North China Craton. *Tectonophysics* 746, 266–279. doi: 10.1016/j.tecto.2017.04.009

Yu, Y., Gao, S. S., Liu, K. H., Yang, T., Xue, M., and Le, K. P. (2017). Mantle transition zone discontinuities beneath the Indochina Peninsula: implications for slab subduction and mantle upwelling. *Geophys. Res. Lett.* 44, 7159–7167. doi: 10.1002/2017gl073528

Zegers, T. E., and van Keken, P. E. (2001). Middle Archean continent formation by crustal delamination. *Geology* 29, 1083–1086. doi: 10.1130/0091-7613(2001)029<1083:macfbc>2.0.co;2

Zhao, D. (2007). Seismic images under 60 hotspots: SEARCH for mantle plumes. *Gondwana Res.* 12, 335–355. doi: 10.1016/j.gr.2007.03.001

Zhao, D. (2017). Big mantle wedge, anisotropy, slabs and earthquakes beneath the Japan Sea. *Phys. Earth Planet. Inter.* 270, 9–28. doi: 10.1016/j.pepi.2017.06.009

Zhao, D., Tian, Y., Lei, J., Liu, L., and Zheng, S. (2009). Seismic image and origin of the Changbai intraplate volcano in East Asia: role of big mantle wedge above the stagnant Pacific slab. *Phys. Earth Planet. Inter.* 173, 197–206. doi: 10.1016/j.pepi.2008.11.009